UNIVERSITY OF CAPE TOWN
IYUNIVESITHI YASEKAPA • UNIVERSITEIT VAN KAAPSTAD

DEPARTMENT OF CIVIL ENGINEERING

TEMPERATURE AND THERMAL STRESS DISTRIBUTION IN CONCRETE ARCH DAMS IN OPERATION

BY:
MERI TONY CARLOS

SUPERVISOR: A/PROF. P MOYO
CO-SUPERVISOR: PROF. MG ALEXANDER

Thesis submitted to the Department of Civil Engineering, Faculty of Engineering and Built Environment, University of Cape Town, in partial fulfilment of the requirements for the Degree of Master of Science (Engineering)

DECEMBER 2011

DEDICATION

To My Loving Mother: Margaret Angwec Oyee

ABSTRACT

The temperature field of concrete dams in operational stages is dominantly influenced by variations in environmental seasonal temperature and climatic conditions. Cyclic seasonal temperature and associated thermally induced stresses have been found to contribute significantly to long term degradation of strength and stiffness of concrete dams raising concerns about their durability (Leger et al. 1993). In this study, a critical review of the current state-of-the-art of temperature models for determining temperature distribution including the main evironmental parameters influencing the temperature distribution for concrete dams in operation has been undertaken. It is found that, the heat flow in the concrete dams currently is approximated as conduction only and the classical Fourier heat conduction models are adopted as the governing equations to define heat flow mechanisms in the dam. The solution to Fourier heat models is accurately achieved through the finite element analysis using finite element models of the dam to the determine the temperature field.

Among the environmental parameters that affect the concrete temperature, the effect of variable foundation and variable reservoir level have been investigated in this study. A model to predict variation in foundation temperature in the absence of measured data is first proposed. A transient heat transfer analysis is then carried out using a hypothetical 3-D finite element model of dam-foundation system to investigate the effect of foundation temperature. Results obtained indicate that spatial variable foundation temperature prescibed at the dam-foundation interface has a significant influence on thermal response of the dam in the regions near the interface. However, variable foundation temperature was found to have negligible influence on the thermal stress response for the selected node at the interface. The reservoir level is found to significantly affect the average concrete temperature by more than 50% for low reservoir level.

ACKNOWLEDGMENT

It goes without saying that a work which attempts to imagine and contemplate on the possible future occurrences in the vanished worlds owes everything to the original literary sources both in material and non- material forms. In this respect, I would like to recognize the works of scholars and other writers; without whom, this work would not have attained the state it has now. It is for their invaluable and immeasurable contribution that I was able, with the help of my supervisor, to develop and produce all that is contained herein; that I consciously looted their extraordinary work and wisdom and used in the process of doing this piece of work

For the development and production of the work itself, I feel greatly honored to extend a deep sense of gratitude:

Firstly to the Almighty God for giving me the strength, health and wisdom to complete this work successfully

To my supervisor A/Prof Pilate Moyo for his academic and kind support, close supervision, guidance and valuable suggestions. I have learnt a lot from his thorough and insightful review of this study and his dedication to achieve high quality and practical research

To my Co-Supervisor Prof Mark Alexander for his academic advice and thorough review of the work

To Concrete and Structural Integrity Research Unit (CoMSIRU) for their financial support during the course of this study which gave me the opportunity to pursue my MSc (Eng) studies in South Africa

Friends and Colleagues especially Bruno Salvodi, Patrick Bukenya, Ssentamu Ivan, Ogwal Boniface, Ebil Patrick, Akol Emmanuel, Kukiriza Esther and most importantly Fualal Sharon for their contribution towards the success of this work

Am also indebted to Dr Denis Kalumba (UCT) and Dr Naku Ziraba (MUK) for making this opportunity fall through

Finally to my Loving Mother, Brother and Sisters for their tireless effort and sacrifice they put in me to realize this dream.

DECLARATION

I hereby declare that this thesis is based on my original work except for quotations and citations which have been duly acknowledged. I also declare that this work has not been previously submitted in any form for a degree at UCT or any other institutions

_____

Meri Tony Carlos

Date:

TABLE OF CONTENTS

LIST OF TABLES

LIST OF FIGURES

LIST OF NOTATIONS

Latin Upper Case

A	amplitude of air temperature fluctuations
A_u	amplitude of resservoir temperature fluctuations
A_o	amplitude of resservoir surface temperature fluctuations
A_m	amplitude of foundation temperature fluctuations
B	strain displacement matrix
B_m	annual mean air temperature
C	capacitance matrix
C_s	Stefan-Boltzmann constant
°C	degree celsius
D_m	material thermal diffusivity
D	generalised material thermal conductivity matrix
$\overline{D}$	stress-strain matrix
E	material elastic modulus
F	vector of nodal force
$\overline{H}$	incident solar energy
H_d	sky diffused radiation
H	depth of reservoir/dam
H_b	beam radiation
H_o	monthly global average of solar radiation on horizontal surface
H_r	ground reflected radiation
I_{sc}	solar constant
[K]	stiffness matrix
K_1	thermal conductivity matrix
K_2	convection matrix
K_3	radiation matrix
K_T	monthly average index of cloud cover
K	degrees Kelvin
L	dam thickness
N	array of shape functions
P	period of cycle
Q	heat source
$\dot{Q}$	rate of heat of hydration
R	Dam radius
T	temperature of concrete
$\overline{T}$	boundary prescribed temperature
T_{ini}	initial temperature state
$\dot{T}$	rate of temperature change
T_a	air temperature
T_w	reservoir temperature

T_m	mean annual reservoir temperature
T_b	reservoir temperature at the bottom
T_t	reservoir temperature at the top/surface
T_g	ground temperature
T_s	ground surface temperature
T_{amb}	ambient temperature
$\overline{T}_{amb}$	mean ambient temperature
T_o	annual mean ground surface temperature
V	wind speed
W	watts
$\overline{Z}$	damping depth of ground temperature oscillations

Latin Lower Case

a	surface absorptivity of solar radiation
b	annual mean reservoir surface temperature
c	material specific heat capacity
$\{d\}$	vector array of nodal temperatures
e	surface emissivity
f	evaporation fraction
h_s	sunrise/sunset hourly angle
h	hourly angle
h_r	radiation coefficient
h_c	convection coefficient
k	material thermal conductivity
$k_x, k_{y,} k_z$	thermal conductivity coeffiecients in x-, y-, and z-directions
m	meters
n	maximum number of time steps
$\vec{n}$	normal vector
p	average coefficient of reflection from surrounding
q	heat flux
q_s	surface heat flux
q_a	heat flux due to solar radiation
q_c	convection heat transfer rate
q_r	radiation heat transfer rate
$\vec{q}$	heat flux vector
$\overline{q}$	boundary prescribed heat flux
r	correction factor for solar constant
r_h	relative humidity
s	seconds
t	time
w	test function
x,y,z	Cartessian coordinate system
y_w	water depth

z	foundation depth

Greek Upper Case

∇^2	Laplacian operator for temperature
ΔR	
Δt	time step length
Γ_T	temperature imposed boundary
Γ_q	flux imposed boundary
Ω	domain

Greek lower Case

α	coefficient of thermal expansion
β	sloping angle of dam surface
δ	solar declination
φ	latitude of location
ω	angular frequency
ε_{th}	thermal strain vector

CHAPTER ONE

1 INTRODUCTION

1.1 Background and overview to study

A significant percentage of existing concrete dams, exhibit some kind of structural deterioration after several years in service (Daoudu et al. 1997). The deterioration is caused principally by thermal effects, with 19 % of reported cases attributed to freezing and thawing and another 9 % to temperature variations (ICOLD 1984).

The transient evolution of the concrete temperature due to seasonal temperature variations plays an important role on the thermal behavior of concrete dams in the operational stages. In order to establish the thermal response, the temperature distributions within the dam and the heat flux exchanges with the environment through the atmosphere (including solar radiation and wind effects), reservoir, and foundation must be evaluated.

Many methods exist to obtain the temperature distributions in concrete dams. The finite difference method (FDM) has been used to obtain the temperature distributions in earlier days. But due to the geometrical complexity of dams and difficulty in handling complex boundary conditions, FDM is reported (Sabbagh-Yazdi and Mastorakis, 2007) to be inaccurate for modeling temperature distribution in concrete dams. The most adopted method for determining temperature distribution in concrete dams is the finite element method (FEM). Several researchers (Leger et al. 1993a; Daoudu et al. 1997; Malla and Weiland, 1999; Sheibany and Ghaemian, 2006; Lababzidah et al.2010) have used finite element analysis to obtain the temperature distribution in dams due to seasonal temperature variations and the corresponding induced thermal stresses. Knowledge of thermal stress is required to periodically assess the structural integrity of concrete dams and perform safety evaluation. It is therefore important to understand how the dam interacts with the environment.

In this study, the influence of the environment to temperature distribution of concrete arch dams is considered. Several factors are known to influence temperature distribution of

concrete dams in operation and they include variable air, water and foundation temperature including solar radiation and wind effects. This research is focused on investigating the effect of spatial variable foundation temperature as well as the influence of fluctuating reservoir level on temperature distribution in concrete dam walls .

1.2 Research Goals

This research aims to contribute to the continuing research efforts on developing practical and suitable models for determining the temperature field and the associated thermal stress in concrete dams in operation. The objectives of the study are as follows :

1. Carry out a thorough literature review of existing current state-of-the-art of temperature models for concrete dams in operation including environmental parameters influencing temperature distribution in the concrete.
2. Propose a foundation temperature model for predicting temperature variations in the foundation.
3. Investigate the influence of the variable foundation temperature and the effect of fluctuating reservoir level on concrete dam temperature distribution.

1.3 Methodology of this study

The research starts with a thorough critical literature review of the current state-of-the-art of temperature models for predicting concrete temperature and factors influencing the concrete temperature . The theory and development of the finite element models are followed to enable develop computer finite element model of the dam used in this study. The implementation of the proposed foundation model is undertaken through a comprehensive transient thermal analysis to establish the influence of spatial variable foundation temperature. The results obtained from the finite element dam model are analyzed and conclusions are drawn and recommendations made based on the study.

1.4 Organization of the study

This thesis contains 7 Chapters. With the present content as introductory Chapter 1. A literature review is provided in chapter 2 and Chapter 3.

In Chapter 2 a comprehensive literature review of the current state-of-the-art of temperature models for determining temperature distribution in concrete dams is done. The review focuses largely on the different temperature models adopted and the implementation techniques. A detailed review to the steps in transient heat flow analysis of concrete dams using Finite element analysis is also included here.

Chapter 3 is devoted to understanding the environmental parameters influencing temperature distribution in concrete dams and how they have been modeled as well as the assumptions considered.

In Chapter 4 a model is proposed for predicting foundation temperature including the factors that influence the foundation temperature.

In Chapter 5 the implementation of the proposed foundation model in finite element model is undertaken following strictly the procedures of heat tranfer process discussed in chapter 2.

The results, analysis and discusions of the study are provided Chapter 6. The convergence of the heat tranfer analysis and the results on temperature and thermal stress are presented.

Finally in chapter 7, conclusions to this study are presented as well as recommendations for further research.

CHAPTER TWO

2 CONCRETE DAM TEMPERATURE DISTRIBUTION MODELS

2.1 Introduction

Many empirical methods and closed form solutions exist to obtain the temperature distribution in concrete dams. In order to obtain accurately the temperature distribution within a dam, an appropriate mathematical model describing the heat flow within the concrete has to be established. Currently, the heat flow within a dam is assumed to be through conduction only (Leger et al. 1993a; Agullo et al. 1996; Malla and Weiland 1999) and hence governed by the transient Fourier heat conduction model.

2.2 Fourier Heat Conduction Model

The Fourier heat conduction equation in a solid region is written generally in cartesian components as:

$$\nabla^2 T + \frac{Q}{\kappa} = \frac{1}{D_m}\frac{\partial T}{\partial t} \qquad [2.1]$$

Where:

$$\nabla^2 = \frac{\partial^2}{\partial x^2} + \frac{\partial^2}{\partial y^2} + \frac{\partial^2}{\partial z^2} \ , \ D_m = \frac{\kappa}{\rho c}$$

∇^2 is the Laplacian operator of temperature, T denotes temperature field T(**x**, y, z, t) and **x, y, z** and t denoting space coordinate vector and time; D_m is the thermal diffusivity of the material; **k** is the tensor which quantifies the conductivity property of the material; c and ρ are material specific heat capacity and density respectively, Q is the internal rate of heat generation in W/m^2.

In transient heat transfer analysis for concrete dams that have been in operation for 10 years or more, the quantity Q is neglected. This is because at this stage, the heat liberation in

concrete wall due to hydration process is assumed complete (Nisar et al. 2003, Saetta et al. 1995). Thus Equation (2.1) reduces to:

$$\nabla^2 T = \frac{1}{D_m}\frac{\partial T}{\partial t} \qquad [2.2]$$

The above is known as the transient Fourier heat conduction equation without internal heat usually applied to determine the temperature distribution in concrete dams in operation. Three forms of Equation (2.2) have been adopted in modeling the temperature distribution of concrete dams: one-dimensional (1-D), two-dimensional (2-D) and three-dimensional (3-D) Fourier heat conduction models.

2.2.1 1-D Heat Conduction Model

In 1-D heat conduction analysis of concrete dams, heat flow is considered only along the thickness (L) of the dam that is in the x direction only. Therefore, the model takes the form

$$\kappa_x \frac{\partial^2 T}{\partial x^2} = \rho c \frac{\partial T}{\partial t} \qquad [2.3]$$

Where: T is the concrete temperature in K; t = time in seconds; k is the concrete conductivity coefficient along x-direction in W/m^2 K.

In Figure (2-1), it is shown that, the concrete dam surfaces are at different temperatures. In applying Equation (2.3), it is considered that heat flows from surface at temperature T_1 to surface at temperature T_2 or vice versa depending on which surface is at higher temperature in accordance with Fourier's law.

The fundamental assumption in using 1-D model is the unidirectional flow of heat which is usually not true especially for concrete dams with considerable thickness (Ardito et al. 2008). This makes the 1-D model in most cases not considered strictly accurate in concrete dams due to the fact that in reality there may be heat flow normal to the x- direction. For this reason researchers in dam engineering have in many cases adopted the 2-D and 3-D heat models.

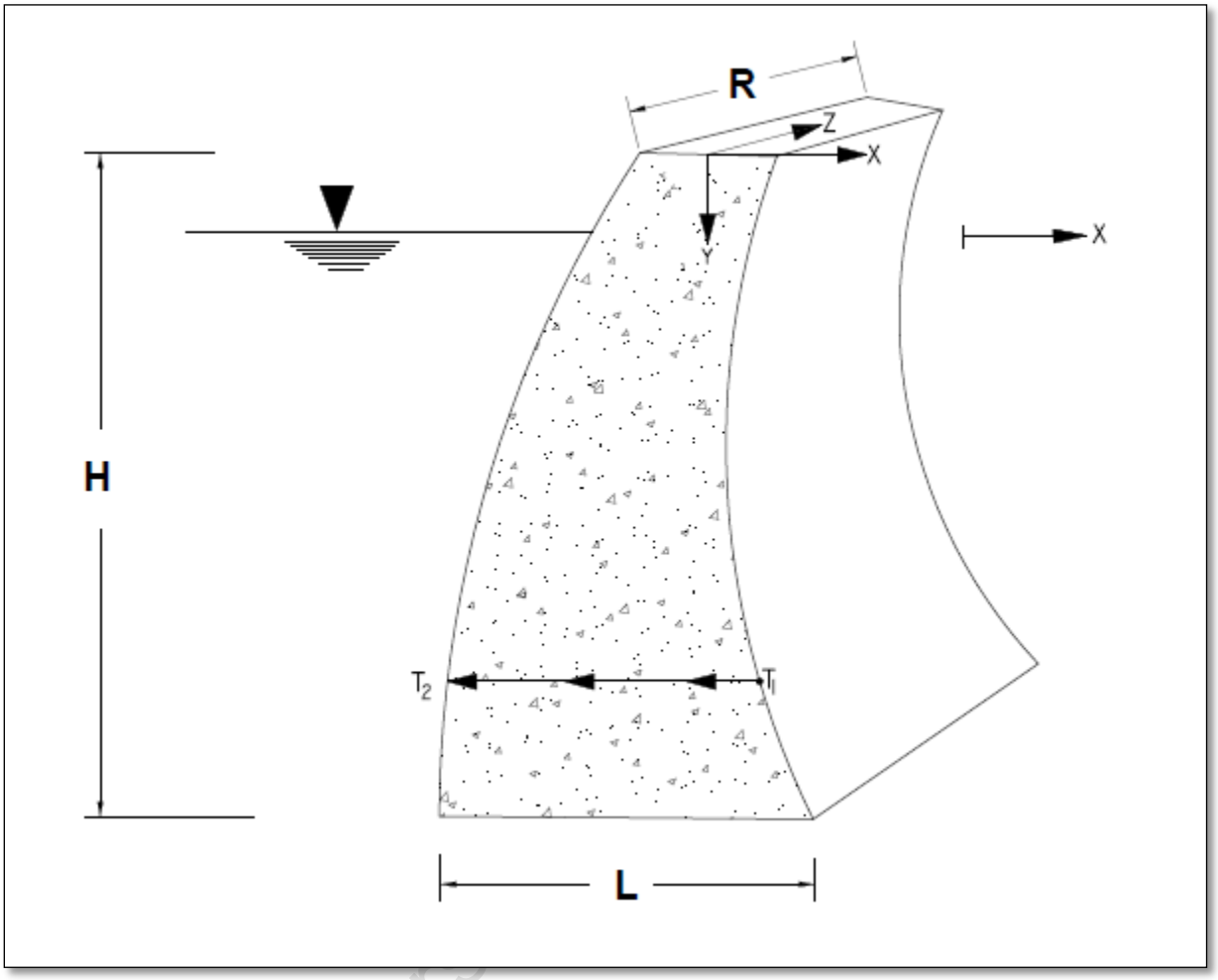

Figure 2-1: 1-D heat transfer in concrete dam wall

2.2.2 2-D Heat Conduction Model

In 2-D heat conduction analysis of concrete dams, heat flow is considered along the thickness (L) of the dam and through the depth (H), that is, heat flow occurs in both x-and y-directions as shown in Figure (2-2). Therefore the model is written as:

$$\kappa_x \frac{\partial^2 T}{\partial x^2} + \kappa_y \frac{\partial^2 T}{\partial y^2} = \rho c \frac{\partial T}{\partial t} \qquad [2.4]$$

Where: T is the concrete temperature in K; k_x and k_y are the concrete conductivity coefficients in x- and y-directions, respectively.

The 2-D heat model can be accurately applied in heat flow analysis of gravity concrete dams as the solar shares on the exposed surfaces of such dams are usually uniform at every point on the concrete surface (Leger et al. 1993; US Army Corps, 1994).

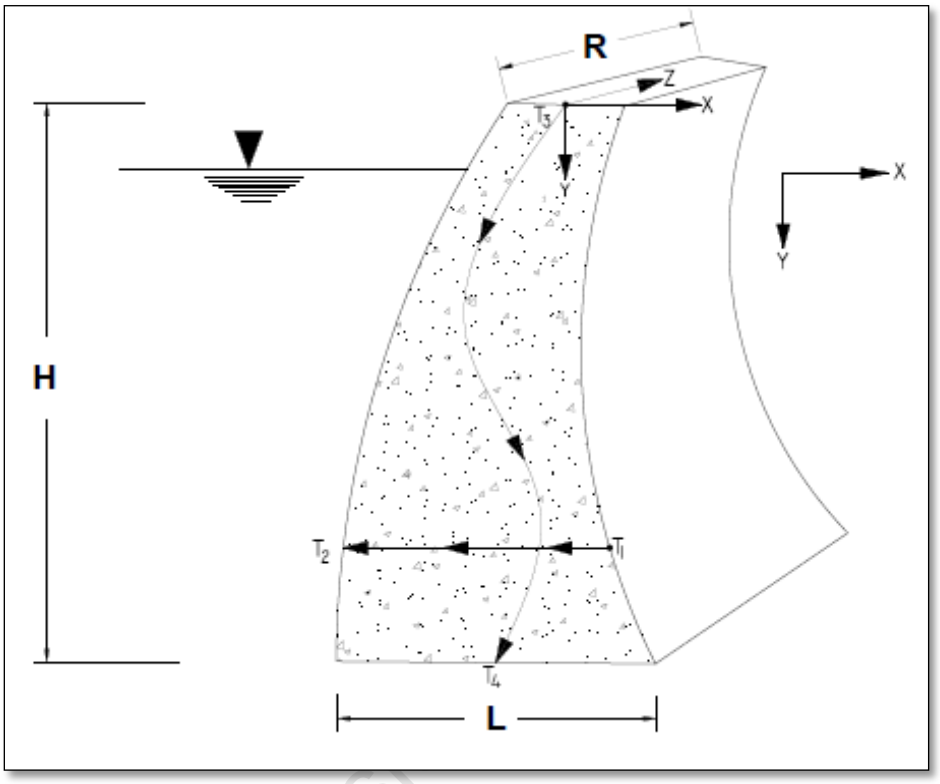

Figure 2-2: 2-D heat transfer in concrete dam wall

2.2.3 3-D Heat Conduction Model

In 3-D heat conduction analysis of concrete dams, heat flow is considered in all three directions that is in the x- , y- and z-directions. In the z-direction, heat flow is assumed across the radius (R) i.e. in the radial direction as depicted in Fig. (2-3). The model therefore takes the form

$$\kappa_x \frac{\partial^2 T}{\partial x^2} + \kappa_y \frac{\partial^2 T}{\partial y^2} + \kappa_z \frac{\partial^2 T}{\partial z^2} = \rho c \frac{\partial T}{\partial t} \qquad [2.5]$$

Where: T is the concrete temperature in K; $\kappa_x, \kappa_y, \kappa_z$ are the concrete conductivity coefficients in x-, y- and z-directions.

The 3-D heat model is the most ideal for thermal analysis of concrete arch dams (Sheibany and Ghaemian, 2006). For an arch dam the sun strikes every point on the concrete surface at different angles and hence there is a spatial variation in the incident solar energy at any location on the concrete surface at a given instant

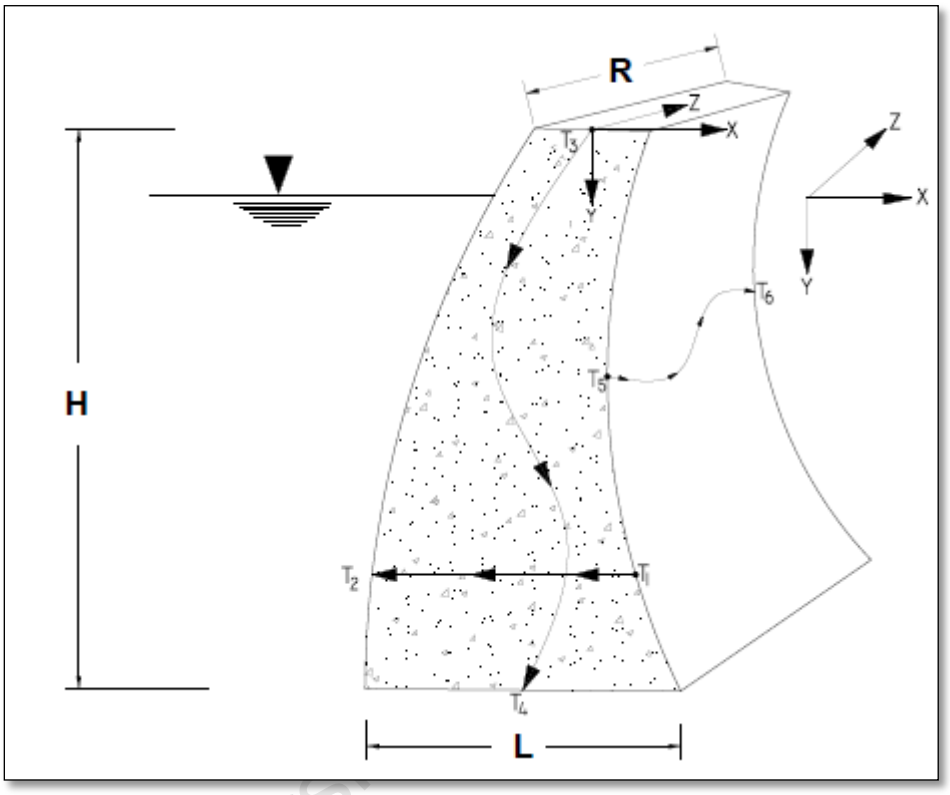

Figure 2-3: 3-D heat transfer in concrete dam wall

2.3 Solution to heat conduction models

Obtaining a solution to heat conduction Equations (2.3-2.5) subject to appropriate boundary conditions means determining temperature distribution, heat flows and conditions of thermal stressing within the structure. In dam engineering this is called thermal analysis or heat transfer analysis or heat flow analysis. The complete solution to the Fourier heat conduction models employs the use of numerical techniques such as finite element method (FEM), finite difference method (FDM), finite volume method (FVM) and Fourier series analysis (FSA) in order to establish the temperature field in the dam.

The finite element analysis (FEA) technique besides its limitations such as large computational effort and required expertise, is currently the most preferred approach to the solution of heat transfer equations. This is particularly due to its ability to deal with irregular geometries and complex boundary conditions and loadings which are the limitations of FDM and FVM. Fourier series analysis on the other hand comes with some advantages over FEM like less computing time requirements and no need for initial temperature condition which is an important requirement when using FEM and FDM (Leger et al 1993; Agullo et al. 1996; Sheibany and Ghaemian 2006)

2.3.1 Thermal analysis using FDM

Before the invention of modern computers, the finite difference method was used to obtain the temperature field. The main idea behind the finite-difference method is that the derivatives in the Fourier heat equations are replaced with the difference formulas (Chapra and Canale, 1998). Agullo et al. (1996) adopted the 1-D heat model to obtain the temperature field of different sections of the dam at given heights and variable thickness at any instant based on explicit FDM. In the analysis, simplified assumptions were considered for instance the concrete medium was assumed continuous, isotropic and homogenous. The influence of thermal properties of concrete, the geometry and location of the dam, and the action of the environment were the major factors considered in the study. The results of the analysis found that the mean temperature of the section depended basically on the annual mean air and water temperature as well as the annual mean total of daily solar radiation at the site and concluded that solar radiation had the greatest effect on the temperature distribution of each section.

At present, FDM is not widely used due to the improved and very reliable commercial finite element analysis (FEA) softwares using high performance digital computers. Additionally, FDM becomes very complicated when dealing with higher dimensions for instance the 3-D case.

2.3.2 Thermal analysis using FSA

This technique is a new approach proposed by a few researchers. Leger and Leclerc (2007) reported that the 3-D nature of heat transfer process across a section of an arch dam can be well represented using the 1-D heat model. In the study, they proposed a frequency domain solution technique that computes the temperature field within the dam cross sections based on discrete Fourier series analysis (FSA). In this technique, two approaches to solving Equation (2-4) were proposed; first approach is by considering the direct problem where temperature histories at the dam surfaces (upstream and downstream) are known. These are then used to calculate the inside temperature field. The second is the inverse problem where temperatures have been measured at selected positions inside a dam wall in order to determine related external boundary temperatures. This was implemented in a computer program called TADAM. From their results, they concluded the proposed technique can be used effectively to study the seasonal thermal variations in concrete dam sections. Another important point was that the accuracy of computed thermal field is independent of the mesh distribution of the section considered which is in contrast to finite element heat transfer solutions.

Ardito et al. (2008) combined both FEM and FSA techniques and proposed a procedure for diagnostic analysis of concrete dams. In the proposed algorithm, FEM discretization process was used to reduce 2-D heat model to first order linear differential equation. Then using Fourier series, an analytical solution of the ordinary differential equation (ODE) was obtained that provided the temperature field over given time period, assuming steady harmonic thermal response of the dam. However, there is uncertainty on the accuracy of this proposed approach as full scale assessment of its validity using real experimental data is yet to be done.

2.3.3 Thermal analysis using FEM

The thermal behaviour and subsequent structural response of typical concrete dams can be represented accurately by 2-D and 3-D models. Presently, the finite element method (FEM) is the widely accepted numerical method for thermal analysis of dams. It must be noted that concrete dams are 3-D structures from a stress stand-point and a 2-D from heat-flow stand-

point (for gravity dams) as little heat is transmitted in the direction normal to the vertical plane i.e. longitudinal through the dam (U.S Army Corps, 1995). Thus in the case where stress response is depended on the thermal output then it is usually in the best interest to use 3-D models in the heat transfer analysis to avoid creating a structural model again.

The methodology for assessing seasonal temperature variation in gravity dams by finite element analysis has been described by Leger et al. (1993a). In the implementation of the proposed methodology, the 2-D heat model was adopted and 2-D FE model developed was used to carry out FEA of a dam-foundation-reservoir system using SAP 90. They took into account different environmental conditions such as ambient temperature variation, solar radiation variations, foundation temperature as well as reservoir temperature changes. The results found that high temperature gradient developed near the exposed surface of the dam may generate tensile stresses capable of causing surface cracking. They did consider foundation in their study assuming adiabatic conditions. This means the thermal interaction between the wall and foundation were ignored. The proposed methodolgy has been adopted and implemented by a number of researchers. Some of the selected research works are reviewed below:

Daoud et al. (1997) combined both Leger et al. (1993a) and Bouzoubaa (1995)'s works and performed numerical analysis on the periodic temperature field in concrete gravity dams using CESAR a finite element commercial program. Contrary to Leger et al (1993a) and Bouzoubaa (1995), they took into account different environmental conditions such as snow cover, temperature gradients and ice formation in the reservoir water, different thermal conductivities for saturated and unsaturated parts of the dam as well as the thermal interaction between the dam and its foundation i.e. considering the effect of geothermal gradient and different temperature profiles in the foundation for both downstream and upstream faces. Results from their study showed a remarkable difference in the temperature gradient at the interface between saturated and unsaturated parts of the dam, that is, temperature gradients are significant in a band of 20 m from its downstream exposed surface and on a vertical distance of 15 m on its wetted upstream side. Based on experimental relations between the

limit of tensile strain of concrete and the local amplitude of seasonal temperature variations, they concluded that thermal effects are significant to a band of approximately 1 m from the downstream exposed surface of the dam. Much as the thermal interactions between the wall and the foundation were considered, the results do not show how much influence foundation temperature has on the over all temperature distribution and the depth of influence zone into the concrete from concrete-foundation interface

Sheibany and Ghaemian (2006) carried out a 3-D FEA to determine the effect of thermal stress in Karaj arch dam adopting 3-D heat equation as the mathematical model. They included in their study the effect of solar radiations as well as other sources of heat generation in dam like air and reservoir temperature changes. Their study found that the effect of water temperature can be more than air temperature in influencing the overall dam's temperature distribution across dam thickness and that solar radiation is the main cause of high temperature variations of points located on the exposed surface especially downstream face. They concluded that 2-D thermal analysis of an arch dam cannot yield accurate results and 3-D numerical simulation is a needed. In this study, the foundation was completely ignored in the model.

Malla and Weiland (1999) investigated the effects of horizontal crack in a concrete gravity arch dam after 25 years in operation using 3-D ADINA finite element model of the dam-foundation system. They considered the effect of thermal load in their study. Their results showed that the daily temperature changes could not be the reason of crack creation as they only affect a very thin layer on the dam surfaces. Comparisons were made with results from 2-D finite element model of the same dam and concluded that the growth of the observed crack could only be explained with a 3-D model. The foundation was included in the model but the effect of foundation temperature was not the objective

Amin et al. (2009) conducted an experimental study in order to simulate the generated stress field due to temperature variations in mass concrete. They provided a numerical simulation using 3-D ADINA FE model to verify and extend the experimental interpretations.

Manafpour et al. (2009) implemented a 3-D finite element model of concrete gravity arch dam and simultaneously examined the effects of thermal loading and earthquakes. They concluded that thermal load was important and can cause crack initiation in dams.

Labibzadeh et al. (2010) carried out thermal assessment of Karun arch dam considering the effect of solar radiation and reservoir temperature changes. Their findings concluded that thermal load is very significant in structural evaluation of the dam.

2.4 Heat transfer analysis process in FEM

In finite element transient heat transfer analysis, three major computational issues ought to be considered. Firstly, is the initial condition (discussed in section 2.4.1) of the dams, the second is related to the numerical integration scheme when a long time behaviour is required and the third is the boundary conditions (details in section 2.4.2).

For an arbitrary 3-D body depicted in Figure (2-4), the governing equation for transient heat transfer is given in Equation (2.5)

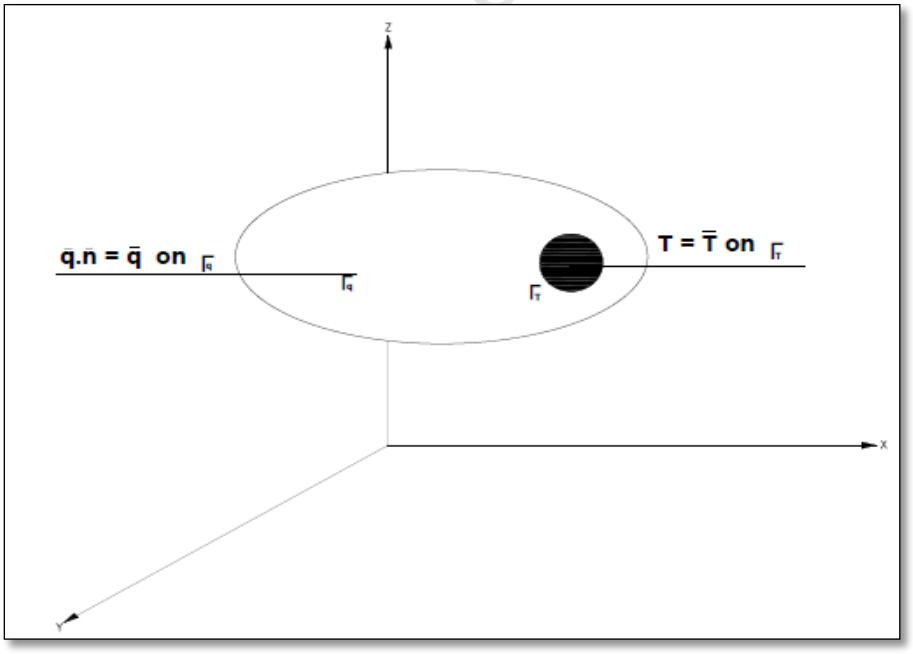

Figure 2-4: A Body subjected to heat transfer

On the surface of the body, the following conditions must be satisfied:

$$T(x,y,z,t) = T_{ini}(x,y,z,t) \qquad \text{on } \Gamma_T \qquad [2.6a]$$

$$\kappa \frac{\partial T}{\partial n} = q_s(x,y,z,t) \qquad \text{on } \Gamma_q \qquad [2.6b]$$

Where: q_s is heat flux, Γ_T is temperature imposed boundary part and Γ_q is heat flux boundary part. Three forms of heat flux contribution to the concrete surface are considered, namely heat flux due to absorbed solar radiation q_a, heat flux due to convection heat transfer, q_c and heat flux due to radiation heat exchange, q_r, between the surrounding medium and the concrete surface. A general expression that describes all the effects is:

$$q_s = q_a + q_c + q_r \qquad [2.7]$$

The initial condition given by;

$$T(x,y,z,0) = T_{ini}(x,y,z) \qquad [2.8]$$

is also prerequisite for the solution of the initial-boundary-value problem given by equations (2.5 – 2.8).

The finite element formulation of equation (2.5) can be derived using the variational principle. The integral form (often called the weak form) is written as;

$$\iiint_{\Omega} (\nabla w)^T D \nabla T \, d\Omega + \iiint_{\Omega} w \rho Q \, d\Omega + \iint_{\Gamma_q} w q \, d\Gamma = 0 \;\; \forall w \text{ with } w = 0 \text{ on } \Gamma_T \qquad [2.9]$$

$$D = \begin{bmatrix} k_{xx} & k_{xy} & k_{xz} \\ k_{yx} & k_{yy} & k_{yz} \\ k_{zx} & k_{zy} & k_{zz} \end{bmatrix}, \; \boldsymbol{q} = -\boldsymbol{D}\boldsymbol{\nabla} T$$

Where Q = heat or thermal source

$q = \bar{q} = -k\frac{dT}{dx}$ on Γ_q, L = dam thickness, D = generalized thermal conductivity, w = test or weight function

For the temperature T within the element, an approximation can be written in the form

$$T = Nd \qquad [2.10]$$

Where N is the array of shape functions and d is the vector of nodal temperatures

After several manipulations of the integral form, the resulting algebraic equation for each element is an ordinary differential equation in time written as:

$$C\dot{T}(t) + \overline{K}T(t) = F(t) \qquad [2.11]$$

If m denotes the number of nodes in the adopted finite element mesh, $\boldsymbol{C}$ and $\overline{K}$ are the (m x m) matrices of thermal capacity and (thermal conductivity + convective + radiative) respectively that is

$$\overline{K} = K_1 + K_2 + K_3 \qquad [2.12]$$

$\boldsymbol{T}$ and F denote the m-vectors of unknown nodal temperatures and nodal force respectively, the latter of which reads in integral form as:

$$F(t) = \int_{\Omega} N^T Q d\Omega - \int_{\Gamma_q} N^T \left(q^T n\right) d\Gamma \qquad [2.13]$$

At the element level

$$C = \rho c \int_{\Omega^e} N N dV \quad ; \; K_1 = \int_{\Omega^e} k B^T B d\Omega \; ; K_2 = \int_{\Gamma^e} h_c N^T N ds \; ; \; K_3 = \int_{\Gamma^e} h_r N^T N ds \qquad [2.14]$$

$$F = \int_{\Omega^e} Q^e N^T d\Omega + \int_{\Gamma^e} q_a N^T ds + \int_{\Gamma^e} h_c T_a N^T ds + \int_{\Gamma^e} h_r T_a N^T ds \qquad [2.15]$$

Where B is the derivative of the shape functions defined as

$$B^T = \left[\frac{\partial N^T}{\partial x} \frac{\partial N^T}{\partial y} \frac{\partial N^T}{\partial z} \right] \qquad [2.16]$$

2.4.1 Initial condition

Initial conditions are conditions for which no thermal load exists in the structure. A concrete dam is subjected to thermal load when the temperature of the concrete exceeds its design temperature causing thermal effects. In FEA of concrete dams, the initial condition is necessary

for the transient temperature field computations. Usually the initial data is not available unless the temperature history of a dam right from construction to its current state is known. The common method for prescribing the initial temperature field is to assume a certain type of steady temperature solution as the initial condition (Venturelli 1992, Leger et al. 1995).

To start transient computations, a steady-state heat transfer analysis is carried out by applying the mean annual air, water and foundation temperatures directly at the boundaries of the model. The mean annual temperature on the downstream face is increased above the mean annual air temperature to account for the effect of solar radiation. This is done for the extreme temperature conditions usually the year with maximum recorded temperature (Leger et al. 1993). Boundary temperature variations of certain periods are repeated in time. When a repetitive temperature time history of a 2 to 3 year simulation is observed, the transient heat transfer analysis is considered to be convergent. Only the results after convergence is achieved seem reliable for practical use. A finite period of the time is required beyond which errors introduced by the assumed initial field temperature to drop to a negligible level.

2.4.2 Thermal Boundary Conditions

The treatment of the boundary conditions in finite element implementation is the most complicated. It is of course very important to prescribe the boundary conditions with the greatest possible consistency, since they have direct influence on the accuracy of the results. The boundary of a dam consists of dam-air boundary, dam-water boundary and dam-foundation boundary. The basic information required to perform a heat flow analysis include; 1) weather data describing the air temperature, solar radiation, wind speed; 2) water temperature 3) foundation temperature; and 4) thermal properties of the materials. Suitable computational models have been established to treat these factors (Leger and Armstrong 1993; Agullo et al. 1996; Ardito et al. 2008). Figure (2-5) shows the heat transfer processes occurring in a dam and the thermal boundary conditions that are usually adopted in thermal analysis of concrete dams.

Concrete-Air boundary

The dam-air boundary is always a difficult problem to deal with. A large difference exists between the temperature of the air and concrete. The heat transfer mechanisms at this boundary are due to radiation and convection. The process is a function of air and concrete temperature, wind speed and solar radiation intensity. Mainly, heat exchanges convectively along this boundary. Difficulties may arise from the determination of the convective coefficient. Because it is a function of air flow, the convective coefficient may be environment dependent. However a larger convective coefficient will make the surface temperature more close to the air temperature.

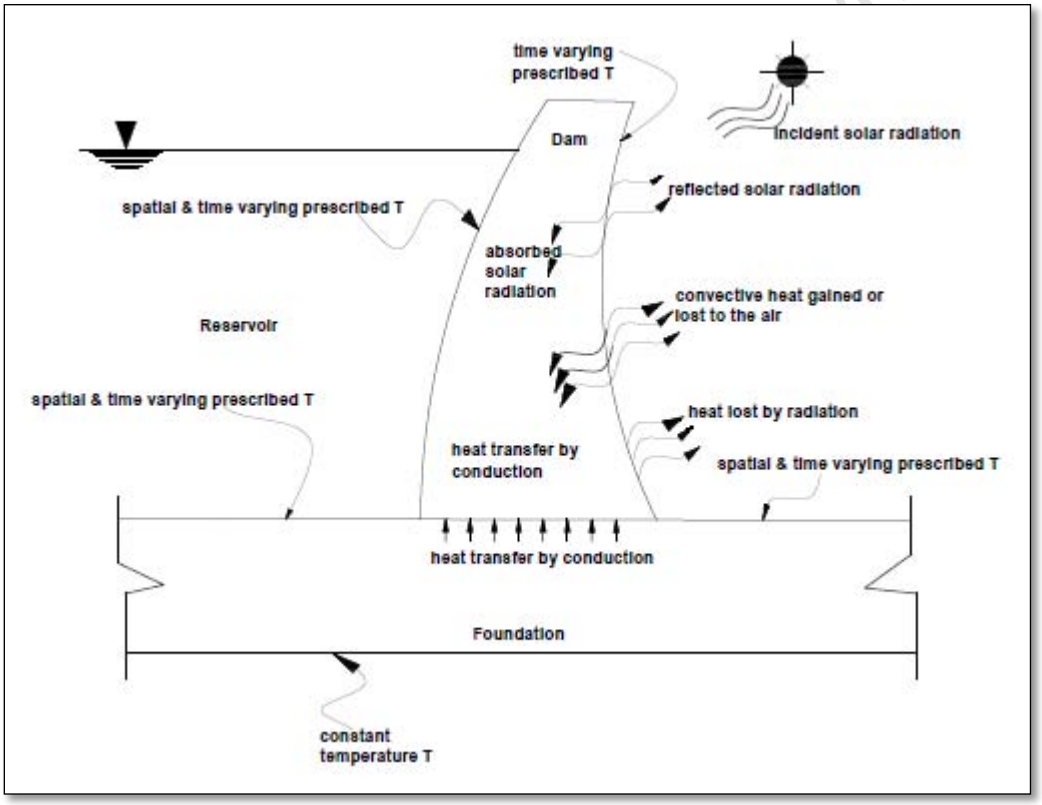

Figure 2-5: Heat transfer mechanism and boundary conditions in concrete dams

Concrete-water boundary

The situation at the water-concrete boundary is similar to that of air-concrete boundary. It is normally assumed in the analysis that the whole upstream face of the dam is completely covered with water to simplify the analysis process. This assumption is well represented in

almost all the past work. This assumption is widely acceptable given the fact that when there is no water on this face then the situation as describe in air-concrete boundary can be applied.

Heat exchanges convectively between the dam and the water (Zhang 1998). For simplicity, Leger et al. (1993) suggested that, for this boundary, the concrete in contact with water can be assumed to have the same temperature as the contact water temperature hence, the dam-water boundary is usually treated as a temperature prescribed boundary (Agullo et al 1996; Daoudu et al 1997; Malla and Weiland 1999; Sheibany and Ghaemian 2006 and Labibzedah et al 2010). This means there is always a small error introduced at this boundary during the analysis (Leger et al. 1993).

Dam-Foundation boundary

At the dam-foundation boundary, there seem to be a lot of uncertainty about what actually occurs. In some cases adiabatic condition is assumed at the interface. This is because concrete is considered a fair insulator hence this kind of simplification does not influence significantly the thermal response away from the interface (Leger et. al, 1993a). In other cases, either temperature or heat flux is prescribed. The prescribed temperature condition has recently been accepted as the most appropriate (Ardito et al. 2008). A detailed review of modeling boundary conditions is provided in Chapter 3.

2.4.3 Time step solution of the FEM equations

Once the initial and boundary conditions have been established the solutions to finite element equations (2.11-2.16) can be obtained. There exist mainly two methods: the mode superposition method and the direct integration method. The method of choice is usually based on whether the long term or short-term solution is required and the scale of the problem.

In order to integrate equation (2-11) with respect to time, the time interval is first divided into equal steps. This is written as:

$$t_o = 0 \text{ and } t_i = i\Delta t, i = 1,.....,n. \qquad [2.17]$$

Where Δt is the time step length and $t_n = n\Delta t$ is the final time of interest and n is the maximum number of steps. The time derivative of the temperature array, $\dot{T}$, at t_{i+1} is approximated by the backward difference scheme, i.e.

$$\dot{T}_{i+1} = \frac{1}{\Delta t}\left(T_{i+1} - T_i\right) \qquad [2.18]$$

Substituting Equation (2-18) into equation (2-11), for time t_{i+1}, we obtain the following difference equation:

$$\left[C + \Delta t\overline{K}\right]T_{i+1} = CT_i + \Delta t F_{i+1} \qquad [2.19]$$

For all the time steps, the matrix $\left[C + \Delta t\overline{K}\right]$ is the same, so that the marching scheme is

$$T_{i+1} = \left[C + \Delta t\overline{K}\right]^{-1}\left[CT_i + \Delta t F_{i+1}\right] \qquad [2.20]$$

Equation (2-20) therefore can be used to determine T_{i+1} in terms of T_i. T_o is actually the initial temperature distribution array T_{ini}. The transient behavior of the concrete can then be determined step by step.

2.5 Thermal stress evaluation

Several algorithms have been proposed for determining the transient thermal stress response due to an arbitrary temperature at the boundary of a monitored structure (Kuo et al.1986; Bimont and Aufort, 1987). In the finite element analysis, the thermal stress response of the dam is determined for every nodal temperature in each element of the domain. Considering the balance of forces, the relationship between nodal displacement vector and the force vector generated by the difference between calculated nodal temperatures and nodal closure/design temperature (i.e. stress free condition), the finite element formulation is given as

$$[K]\{d\} = \{F\} \qquad [2.21a]$$

$$K = \iiint_{\Omega_e} B^T \overline{D} B d\Omega \qquad [2.21b]$$

$$F = \iiint_{\Omega_e} B^T \bar{D}\ _{th}\ \Omega \qquad [2.21c]$$

$$\varepsilon_{th} = \alpha\left(T - T_{ini}\right) \qquad [2.21d]$$

Where **K** = stiffness matrix, $\bar{D}$ = stress-strain matrix, **B** = strain displacement matrix, **d** = nodal displacement vector, ε_{th} = thermal strain vector, **T** = calculated nodal temperature; T_i = nodal initial temperature; and **α** = coefficient of thermal expansion.

Under long-term action of stress, creep will give rise to an increase in the concrete strain, relieving some of the induced static stresses. The concrete creep mechanism depends on several factors like age of the structure at loading, the duration and time variation of loadings, temperature and humidity. A rigorous stress-creep-temperature interaction analysis which is beyond the the scope of this study. To obtain realistic results, based on suggestions from previous works (Leger et al. 1993a; US Army Corps of Engineers,1995), it is assumed that the long term temperature stress will be 65% of the results obtained by the short term linear elastic analysis.

Concrete cracking is assumed to occur when the tensile stress from combined action of all the loading conditions are exceeding its tensile strength. Generally the tensile strength of concrete used in dam construction ranges from 1.5 MPa to 3.5 MPa (Leger et al. 1993b).

2.6 Thermal stress analysis procedures in FEM

The transient evolution of concrete temperature plays an important role in the thermal behavior of concrete dams from the construction stages where the dissipation of the heat of hydration is dominant and later during operational stages where the cyclic seasonal temperature variations are dominant.

In order to establish the thermal response, the temperature of the dam and the heat flux exchanges with the environment through the atmosphere (including solar radiation and wind effects), reservoir, and foundation in as far as this affects the concrete temperature, must be considered.

Seasonal thermal effects can be included in structural analysis using different modeling techniques as described below;

a) Carry out a coupled thermo-elastic analysis which deals simultaneously with temperature and Stress/displacement. This is only performed if the stress and temperature results are strongly dependent. Material modeling includes temperature dependence of all parameters, anisotropic thermal conductivity, gap conductance and radiation. However, it should be noted that this approach is rather expensive to perform numerically as it requires detailed information about the 3-D thermal history of the concrete surfaces that is usually unavailable

b) Perform a sequentially coupled thermal analysis to define critical temperature distribution that can be used as input for the stress analysis model. This is possible if temperature history is considered without knowledge of stress history of the structure. This means that a separate thermal analysis is performed and the results imported in the subsequent stress analysis. It is therefore advised here that the same model used for thermal analysis must be used for stress analysis to minimize generating significant errors from model modification or generating input data. This approach takes advantage of simple basic assumptions of the structure such as semi-infinite solid and linear or sinusoidal variations of thermal boundary conditions that will lead to closed form analytical solutions to approximate the temperature gradient within the section.

c) If extensive measured internal and external temperature field data are available, direct interpolation can be performed to define the isothermal contours at different times of the year. These results can then be applied to the stress model. Again this approach has the disadvantage that huge thermal database is required to obtain meaningful results which are not generally available

2.7 Summary

The heat flow in concrete dams is governed by the Fourier heat conduction equation. The Fourier heat equation takes three forms these are the 1-D, 2-D and 3-D heat conduction equations.

The fundamental assumption in using 1-D model is the unidirectional flow of heat which is usually not true especially for concrete dams with considerable thickness. This makes the 1-D model in most cases not considered strictly accurate in concrete dams due to the fact that in reality there may be heat flow normal to the x- direction. For this reason researchers in dam engineering have adopted the 2-D and 3-D heat models.

Several solution technique are available to obtain solution to the heat conduction models. But the reliability of these techniques are not very well known. For instance FDM requires the use of structured grids for geometric discretization which affects the accuracy of the result especially when dealing with spherical or curved surfaces. Besides the errors obtained as result of conversion of the differential form of the governing equation to simple formulations that degrades the accuracy of the numerical solution, the method also makes it difficult to model domains with complex geometries and boundary conditions.

The finite element 2-D models may be considered accurate enough for concrete gravity dams; but for concrete arch dams where solar radiation effects vary from point to point on the dam surface then the 3-D models must always be used

The discussions involving foundation temperature and its influence on concrete temperature profile is less convincing in the literature hence a more detailed understanding is required to assess its impact on thermal response of the structure.

CHAPTER THREE

3 ENVIRONMENTAL PARAMETERS

3.1 Introduction

During and immediately after the construction phase of a dam, the most important factor influencing temperature distribution is the heat liberated by the hydration of cement (Abdallah et al. 2003; Saetta et al. 1995). After the construction phase, a regular periodic change in temperature of the dam gradually appears. This is due to variable environmental conditions such as air temperature, reservoir temperature as well as solar radiation shares on the exposed concrete surface (Leger et al. 1993a; U.S Army Corps, 1995; Agullo et al. 1996; Abdullah et al. 2003). After a period of about 10 years post construction, temperature changes in the dam are controlled by the thermal action owing to the surrounding environment and exposure to solar radiation. Figure (3.1) shows the environmental parameters influencing the temperature distribution in concrete dams in operation.

Accurate prediction of concrete dam's temperature distribution therefore requires a good understanding of thermal interaction of the dam and its environment.

The modeling of the concrete heat exchange with the environment is dependent on the surrounding features such as concrete wall and ground surfaces, ambient conditions (i.e air,water and foundation temperatures) , orientation of the dam and heat conduction from the concrete interior. Particularly radiation and convection on the exposed dam surface are dependent on these parameters. Radiation exchange with the environment involves incoming and outgoing components. Solar radiation, radiation from the atmosphere and radiation from the surrounding surfaces can all impact the surface temperature of the concrete wall. Convection on the outside of the dam wall consists of free and forced convection. Free convection is the heat transfer due to bulk fluid movement (due to buoyancy forces from the temperature differences in the air during heat exchange) and diffusion of the fluid around the concrete surface. Forced convection is the heat transfer from bulk fluid movement caused by the wind.

It must however be noted that the major form of heat transfer occurring at the concrete surface is heat conduction and hence governed by Fourier‘s law.

Below is a brief description of the environmental parameters and the boundary condition models that have been adopted in most thermal analysis of concrete dams using finite element implementation

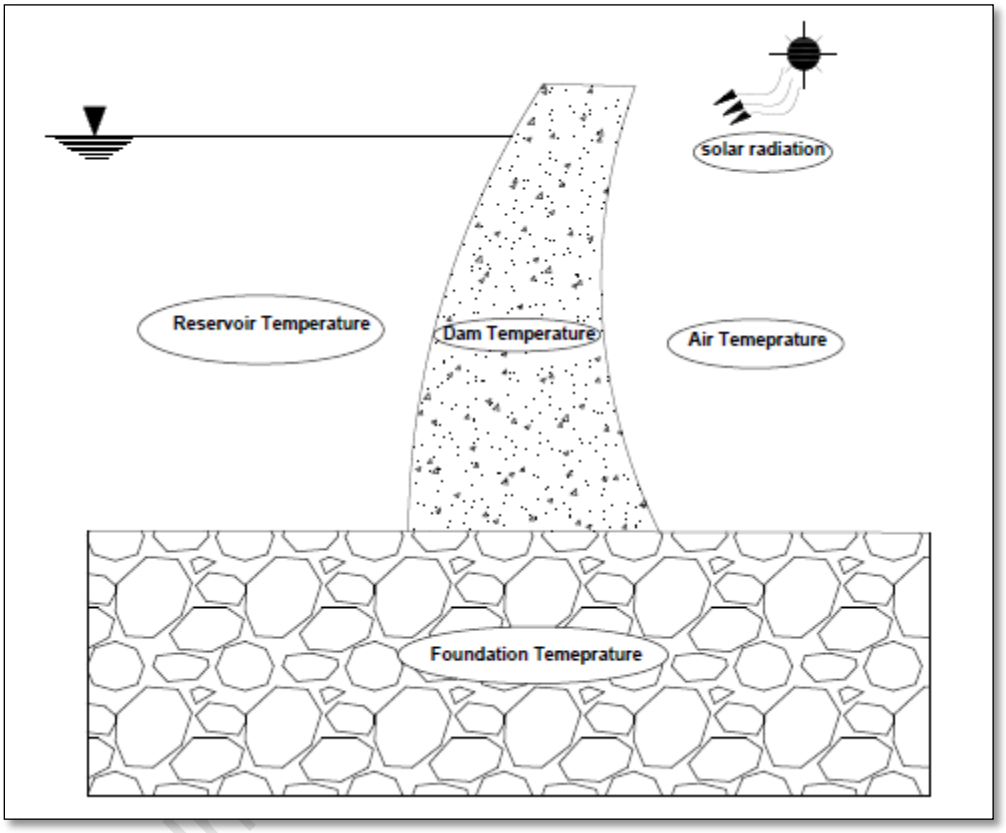

Figure 3-1: Factors influencing concrete dam temperature distribution

3.2 Solar radiation

Solar radiation is an important source of thermal load reaching the exposed surfaces of a dam. It raises the temperature of the concrete surface resulting in the concrete surface temperature to be above that of the surrounding air especially during high or summer temperature conditions (Daoudu et al. 1997). The amount of incident solar reaching the exposed concrete surface depends on the time of day (daily), time of year (season), latitude of the location,

nature of concrete surface, cloud cover and local topography. Other factors such as orientation of dam surface may also have a significant effect on the amount of radiant heat reaching the dam especially in the case of arch dams .

3.2.1 Solar radiation model

Solar radiation energy incident on the concrete surface is either reflected or absorbed by the surface. The total amount of incident energy per unit area per unit time is denoted by $\overline{H}$. The portion of this total incident energy per unit area per unit time that is absorbed by the concrete surface is denoted by q_a. The fraction of the total incident energy that is absorbed is referred to as the absorptivity, a. Therefore, the amount of solar energy absorbed by the concrete surface q_a, may be obtained as

$$q_a = a.\overline{H} \qquad [3.1]$$

$\overline{H}$ is dependent on direct/beam, diffused and reflected components of solar radiation and is obtained from:

$$\overline{H} = H_{b,h} + H_{d,h} + H_{r,h} \qquad [3.2]$$

Where

$H_{b,h}$ hourly direct radiation reaching the concrete surface from the sun

$H_{d,h}$ hourly diffused radiation reaching the concrete surface after it has been scattered by the atmosphere

$H_{r,h}$ hourly ground reflected solar radiation onto the concrete surface (see Fig: 3-2)

Usually these data are in most cases not available hence the data that is commonly used to obtain the amount of incident solar radiation on dam surface pertain to the monthly average of the daily global solar radiation on horizontal surface (H_o).

Using the monthly average H_o, the amount of daily sky diffused radiation (H_d) is calculated and subsequently, the beam radiation (H_b) is obtained as (Liu and Jordan, 1967):

$$H_b = H_o - H_d \qquad [3.3]$$

The relation between H_o and H_d is expressed as

$$H_d = H_o(1.39 - 4.027K_T + 5.531K_T^2 - 3.108K_T^3) \quad [3.4]$$

Where K_T is the index of the average monthly cloudiness, defined by the ratio between H_o and the monthly average of extraterrestrial solar radiation H_e

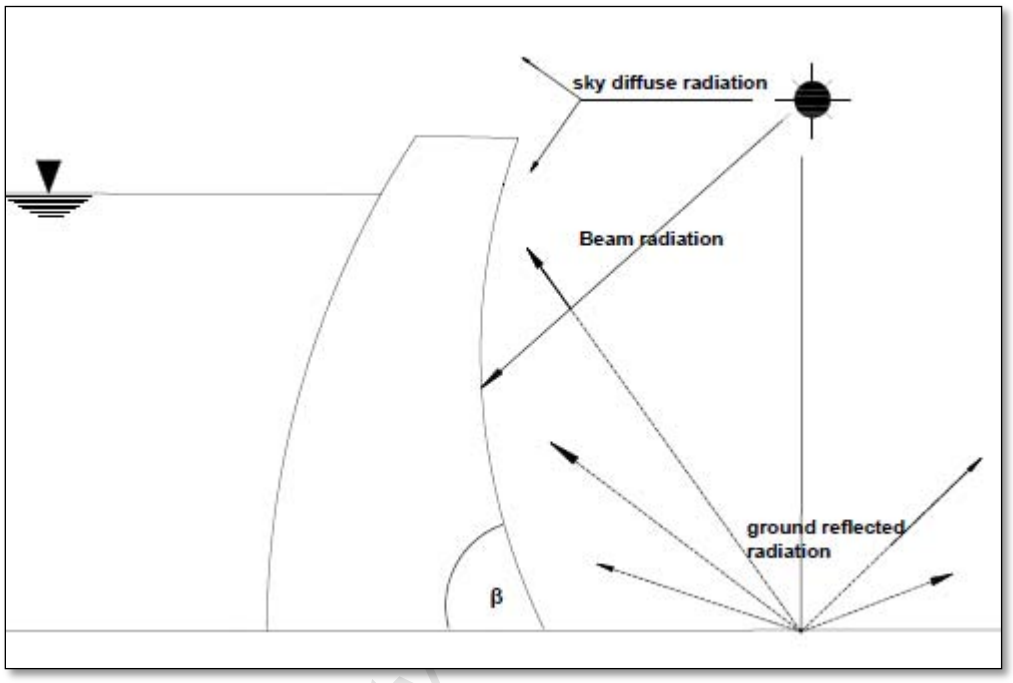

Figure 3-2: Beam, sky diffuse and ground reflected radiation

$$K_T = \frac{H_o \pi}{24 r^2 I_{sc}(\cos\varphi \cos h \sin(\quad)_s \delta + \sin\varphi \cos \quad)} \quad [3.5]$$

Where, r^2 is the correction factor of the solar constant for every day of the year

$$r^2 = 1 + 0.003\cos(\frac{360Z}{365}), 1 \le Z \le 365$$

Where

I_{sc} = solar constant (its value is 4870KJ/hm^2), δ = solar declination, φ = latitude of dam location

h_s = absolute value of the hourly angle of corresponding to the sunset, expressed in radians

The solar declination can be obtained from tables or approximate formulas that express the declination as a function of the day of the year for example the one proposed by Duffie and Beckman (1974). In order to calculate the declination δ, a representative day is taken to be that when the extraterrestrial radiation is closest to the value of the average daily extraterrestrial radiation during a given month. In Table 3-1, the representative day for every month and corresponding value of the solar declination are presented (Coronas et al. 1982)

The hourly angle (h_s) corresponding to the sunset is obtained from

$$\cos(h_s) = -\tan\delta.\tan\varphi \qquad [3.6]$$

Where ($-h_s$) is hourly angle that corresponds to sunrise

Knowing the hourly angles of sunrise and sunset, the duration of the solar day (TSV) can be determined. This duration is the time between two consecutive passes of the sun over the longitude of the location. The relation between TSV (in hours) and the hourly angle (in degrees) is given by

$$h_s = 15(TSV - 12) \qquad [3.7]$$

Consequently, the beginning of solar day (TSV_i) and the end of solar day (TSV_e) are given by the relations below:

$$TSV_{i,e} = 12 \mp \frac{1}{15}\left(\cos^{-1}(-\tan\delta.\tan\varphi)\right) \qquad [3.8]$$

Table 3-1: Mid-day and their solar declination

Month	Middle day	Degrees
January	17	-20
February	15	-12.7
March	16	-1.7

April	15	9.8
May	15	18.9
June	10	23.0
July	17	21.2
August	17	13.4
September	16	2.6
October	16	-8.9
November	15	-18.5
December	11	-23.0

$$TSV_e(\varphi) = 12 - \frac{1}{15}\left(\cos^{-1}(-\tan\varphi.\tan\delta)\right) \qquad [3.9]$$

$$TSV = (TSV_e(\varphi) - TSV(\beta)) = \frac{2}{15}\left(\cos^{-1}(-\tan\varphi.\tan\delta)\right) \qquad [3.10]$$

The above relations (3.8-3.10) depend on the latitude φ of dam location and the day of the year (Z). Thus for a given dam the interval of the solar radiations at its location can be determined. Outside this interval, the incident solar radiation is taken to be zero.

Once the direct and diffuse components of the monthly average of the daily global radiation at the location (horizontal plane) have been determined, we can also obtain the hourly radiation at different times during the interval that corresponds to sunrise and sunset at the location of the dam.

The hourly radiations for global and diffuse are obtained by the relations

$$H_{o,h} = r_t . H_o \qquad [3.11]$$

$$H_{d,h} = r_d . H_d \quad [3.12]$$

r_t and r_d are factors depending on hour and duration of the day, and are obtained analytically as

$$r_d(h, h_s) = \frac{\pi}{24} . \frac{\cosh - \cosh_s}{\sinh_s - h_s . \cosh_s} \quad [3.13]$$

$$r_t(h, h_s) = \frac{\pi}{24}(a_1 + a_2 \cosh) \frac{\cosh - \cosh_s}{\sinh_s - h_s \cosh_s} \quad [3.14]$$

$$a_1 = 0.4090 + 0.5016 \sin(h_s - 1.047)$$

$$a_2 = 0.6609 - 0.4767 \sin(h_s - 1.047)$$

The direct hourly radiation is obtained, at every hour of the interval, as the difference of the hourly global radiation and diffuse radiation as

$$H_{b,h} = H_{o,h} - H_{d,h} \quad [3.15]$$

From the direct and diffuse components of the solar radiation, the amount of incident solar radiation of the dam surface is computed as the sum of their hourly beam, diffuse and reflected components

$$\overline{H} = H_{b,h} + H_{d,h} + H_{r,h} \quad [3.16]$$

Where ground reflected radiation $H_{r,h}$ is given as

$$H_{r,h} = p\left(\frac{1 + \cos\beta}{2}\right).(H_{d,h} + H_{b,h}) \quad [3.17]$$

3.2.2 Surface irradiation model

Concrete surface emits radiation as part of the heat transfer process. Radiant heat transfer rate from a concrete surface to its surroundings is governed by Stefan-Boltzmann law as

$$q_r = e_c C_s (T^4 - T_a^4) \quad [3-18]$$

Where q_r is the heat lost from the concrete surface per unit area per unit time; e_c is the emissivity of concrete surface; a factor obtained as the ratio of total radiant energy emitted by the concrete surface to that emitted by a black body. The emissivity term accounts for the efficiency of the surface in emitting radiation and depends on the concrete surface temperature and colour (Incropera and Dewitt, 2002). *e* is dimensionless constant and takes a maximum value of 1.0. T being temperature of the concrete surface (i.e. this quantity must be known either from recorded data or obtained from steady state analysis as explained in section 2.4.1); T_a is the air temperature (see section 3.6.4), C_s = Stefan-Boltzmann's constant given by 5.669 X 10^8 (W/m^2)

In linear form;

$$q_r = h_r(T - T_a) \qquad [3.19]$$

Where *hr* is defined as linearized radiation coefficient (W/m^2)

$$h_r = e_c C_s(T^2 + T_a^2)(T + T_a) \qquad [3.20]$$

3.2.3 Convection model

Heat is transferred to and from the concrete surface to the surrounding fluid by convection. Convection at the concrete surface is governed by Newton's law of cooling given as

$$q_c = h_c(T - T_a) \qquad [3.20]$$

Where:

h_c = convective heat transfer coefficient; T = temperature of concrete surface (K) ; T_a is air temperature (K). The convective heat transfer coefficient (h_c), defines, in part, the heat transfer due to convection. The convective heat transfer coefficient is sometimes referred to as a film coefficient and represents the thermal resistance of a relatively stagnant layer of fluid between a heat transfer surface and the fluid medium. Common units used to measure the convective heat transfer coefficient are W/(m^2.K).

In concrete dams, the convection can be considered a combination of free and forced convection. In free convection, the bulk fluid motion is caused by buoyancy forces from

differences in local fluid density. The local fluid density gradients are caused by local heating or cooling of the fluid in contact with the surface. If the boundary layer air is heated by the concrete surface, the air's density will be lowered and the air will travel up the dam wall. In forced convection, the fluid motion is caused by an external source of fluid motion. The wind will move the air around the surface, creating forced convection.

The heat coefficient h_c, is a function of wind velocity and can be related to it empirically as proposed by several authors as:

$h_c = 3.83V + 4.67$ (Kehlbeck, 1975) [3.21a]

$h_c = 3.8V + 5.7$ (Kreith and Kreider, 1981) [3.21b]

$h_c = 3V + 2.8$ (Duffie and Beckman, 1980) [3.21c]

Where V is the wind speed at the dam location in m/s

3.3 Air temperature

The daily and seasonal air temperature variation is largely due to the horizontal movement of air, resulting from movement of relatively cold or warm air masses. Other factors which can greatly influence air temperature are physical processes such as absorption and emission of radiation, heat conduction near concrete surface.

3.3.1 Air temperature model

Estimates of the air temperatures at a dam sites are made based on recorded data. Researchers have observed that, air temperature at the dam site varies in an almost sinusoidal fashion over given period of time (Leger et al. 1993a; Agullo et al 1996; Sheibany and Ghaemian 2006) and hence can be approximated by;

$$T_a = A\sin\left[\frac{2\pi(t-\xi)}{365}\right] + B_m \quad [3.22]$$

A = amplitude in °C ; B_m = annual mean temperature in °C; t = time in days; ξ = lag factor of sinusoidal representation of daily temperature

The amplitude of the sine wave, *A*, can be determined by the following

$$A = 0.5\left(\left|T_{\max} - T_{mean}\right| + \left|T_{\min} - T_{mean}\right|\right) \quad [3.23]$$

T_{max} = maximum average monthly temperature, T_{min} = minimum average monthly temperature, T_{mean} = yearly mean average temperature

3.4 Reservoir temperature

The temperature of the concrete wall will greatly be influenced by the temperature of the impounded water. Reservoir water temperature varies with depth and follows a cyclical seasonal variation. Variations in reservoir water temperature depends on many environmental variables including seasonal meteorological cycles; water depth; intensity of wind; air temperature; inflow of water and the reservoir operating conditions. Reservoir water temperature fluctuates on a daily and seasonal basis. Surface conditions are always assumed to cause water temperature to fluctuate in time and depth (Leger et al. 1993). Kauffman and Thompson (2005) analyzed the effect of solar radiation, rain, wind, humidity, and air temperature on water temperature at different depths and the periods of time over which high or low temperatures persisted. Their result showed significant temperature fluctuations at 1 m, 2m, 4m and 10m depth from the investigated sites. At 20 m depth however, the daily signals were very weak and temperature fluctuation recorded was as low as 0.2 °C. They concluded that although the annual range of temperatures were similar at all depths, there was a substantial difference in the rate and frequency of temperature changes at each depth that is at all sites, temperature fluctuations were greater and more frequent at shallower depths.

3.4.1 Reservoir temperature model

Temperature of the impounded water is a function of time and depth of the reservoir. There is no general rule to define reservoir temperature profile. Closed-form expressions to obtain the reservoir temperature profile and its variation with time have been suggested by Bofang and Zhammei (1990) and Ardito et al. (2008). Two types of reservoirs with different temperature profiles are generally recognized (Leger et al. 1993a). The first type is formed by deep reservoirs with small water intake with respect to volume (Fig. 3-3). The second type has an important inflow of water with respect to their volume and is usually shallower. In shallow bodies of

water, energy from the sun is able to penetrate to the bottom and heat the entire water column; thus nearly uniform temperature profile is expected. Deep bodies of water however may become stratified, with warmer, less dense, water floating on top of colder, denser, water near the bottom.

In the absence of measured reservoir temperature, the empirical model suggested by Bofang and Zhanmei (1990) can be used to predict the water temperate in heat transfer analysis. The proposed empirical formula provides the water temperature as a function of time *t* and water depth y_w below the reservoir level and is writen as

$$T_w(y_w,t) = T_m(y) + A_u(y)\cos\left(- _o - \right) \qquad [3.24]$$

t is time in days; y_w is the water depth; T_m is the annual mean temperature of water obtained as $T_m = c_o + \left(b - c_o\right)e^{-0.04y_w}$; $c_o = \dfrac{T_b - bg}{1-g}$; $g = e^{-0.04H}$ T_b is the water temperature at the bottom; b is the annual mean water temperature at the surface of the reservoir; H is the depth of the reservoir; $A_u(y_w)$ is the amplitude of annual variation of water temperature given by

$A_u(y_w) = A_0 e^{-0.018y_w}$ where A_0 is the amplitude of annual variation of water temperature at the surface of the reservoir; t_o is the time of maxmum air temperature; ξ is the phase difference between the maximum temperatures of water and air

Equation (3.24) was slightly modified by Ardito et al. (2008) which makes use of measured water temperature. The modified form is given as

$$T_w(y_w,t) = T_b(t)\frac{1-e^{-\Phi y_w}}{1-e^{-\Phi H}} + T_t\frac{e^{-\Phi y_w} - e^{-\Phi H}}{1-e^{-\Phi H}} \qquad [3.25]$$

Where T_b and T_t are time sequence of temperature measurements at y_w = H and y_w = 0 respectively and Φ represents an empirical parameter which must be evaluated for the dam under investigation (for instance Bofang and Zhanmei proposed $\Phi = 0.04$ for their situation).

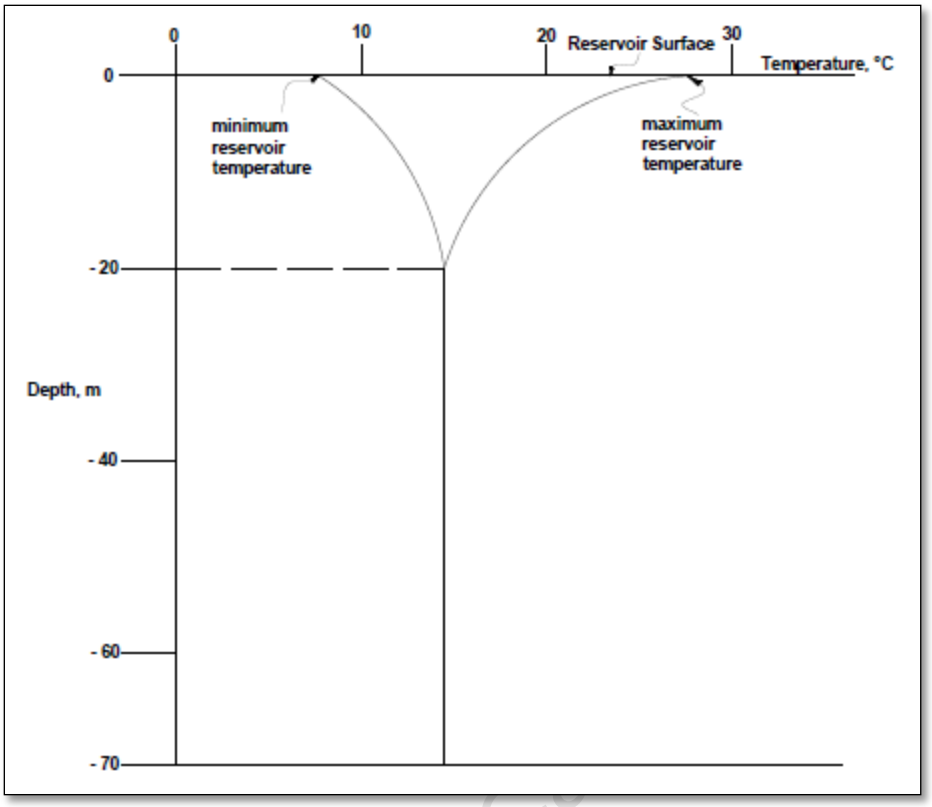

Figure 3-3: Reservoir temperature profile (deep reservoir)

3.5 Foundation temperature

The influence of foundation temperature to temperature distribution of concrete dams in most thermal analysis cases found in literature is far less convincing . Leger et al. (1993b) reported that the foundation temperature has no effect on the concrete away from the foundation surface but they do not show the influence zone into the concrete. Similarly Daoudu et al. (1997) considered the effect of geothermal gradient and their report does not include how much foundation temperature influences the concrete temperature. In this study we investigate the influence of foundation temperature to concrete temperature showing the area of influence into the concrete wall from the dam-foundation interface.

3.5.1 Foundation temperature model

While data and empirical models are available to predict the climatic conditions at dam site, there is lack of data and models available to accurately predict foundation temperatures.

Researchers have often ignored foundation in the finite element model (Agullo et al. 1996; Sheibany and Ghaemian 2006) or included it and assumed an adiabatic condition (Leger et al 1993a) at the dam foundation interface in the thermal analysis of concrete dams. In Chapter 4 we present in details the factors that influence foundation temperature and propose a model that can be easily used to predict the variation in foundation temperature.

3.6 Summary

The seasonal variations in air, reservoir and foundation temperature as well as solar radiation including wind effects are responsible for temperature field in concrete dams in operational stages.

Solar radiation is an important source of thermal load reaching the exposed surfaces of a dam. The factors that influence the amount of incident solar reaching the exposed concrete surface are; time of day, time of year, latitude of the location, nature of concrete surface, cloud cover and local topography. Other factors such as orientation of dam surface may also have a significant effect on the amount of radiant heat reaching the dam especially in the case of arch dams. All these factors need to be incorporated in thermal analysis of dam if realistics results are to be achieved. However inclusion of all these makes the analysis rather complex and difficult to deal with especially in the case of different seasons having variable solar heat reaching the dam surface.

Mathematical models such as solar, irradiation, convection models described here in are put forward to simplify thermal analysis of dams in respect of solar effect on dam temperature.

Air temperature time at dam site generally varies sinusoidally for a given period of time. Major factors influencing air temperature are the time and season of the year in which extreme hot and cold air particles dominate in the summer and winter seasons respectively. The influence of air temperature to concrete dam temperature distribution is more prominent near the exposed surface.

To fully understand the influence the effect of water temperature on concrete dam temperature distribution is not an easy task. A number of complex mechanisms occur at the

dam-water interface which are difficult to analyse. Such factors convection, raditon and conduction are complex to handle at this interface. For that matter reservoir models presented here approximates water temperature which is subsequently used to represent concrete temperature at that boundary for easy of implementation in thermal analysis. Among the different factors that influence water temperature, water depth and seasonal metereological cycles are considerably the most influencial. The water temperature changes with depth in the different seasons of the year.

The discussion involving foundation temperature and its influence is not adequately given in detail to sufficiently draw conclusions. With this, a comprehensive detailed analysis of the factors that influence foundation temperature and its influence is presented in the chapters to follow including a mathematical model to predict foundation temperature is suggested.

Finally, the environmental parameter models presented here are only adopted to perform thermal analysis in the case where measured records are not available. However if reliable measured records of these parameters are available they should be used instead.

CHAPTER FOUR

4 FOUNDATION TEMPERATURE

4.1 Introduction

The temperature field in a dam is influenced by a number of factors including foundation temperature. However, following the literature review, it was clear that the discussions involving the effect of foundation temperature to temperature distribution in the concrete wall is far less convincing. In addition models have been established to predict variation in the other parameters but for foundation is lacking. In this chapter, the factors that influence the foundation temperature are discussed and a model is proposed to predict variations in the foundation temperature

4.2 Factors influencing foundation temperature

Leger et al. (1993a) reported that the depth of penetration of annual atmospheric temperature in the foundation is assumed to be 10m, below this, the ground temperature increases due to the geothermal gradient. Two factors are therefore considered to influence foundation temperature;

- Geothermal energy
- Variable atmospheric temperatures

4.2.1 Geothermal energy

Geophysical studies have revealed that the Earth has several distinct layers at different temperatures as seen in Table 4-1. The core is considered to be the hottest and thus radiates heat to the upper layers. Consequently, a current of heat flows from the core through the mantle to the crust. These are known as the convection currents. This current cools down as it comes closer to the surface of the earth due to the cooling effect provided by the atmosphere. This means that there is always constant flow of heat from the hot center to the surface. This creates a geothermal gradient that depends on the thermal conductivity of the bedrock. As one

moves from the surface to the core however, the temperature gradient decreases with depth. This is due to;

i. Radioactive heat production which is concentrated within the crust of the Earth, particularly within the upper part of the crust, as highest concentrations of uranium, thorium and potassium are found here. These three elements are the main producers of radioactive heat within the Earth.

ii. The mechanism of heat transfer changes from conduction, as within the rigid tectonic plates, to convection in the portion of Earth's mantle that convects.

Research has shown that temperature increases at a rate of approximately 30 ^{o}C/km in the upper crust. This is estimated to occur in the first 10 km from the earth surface as shown in Figure (4-1). Below 200 km from Earth surface, the temperature increase rate decreases to only approximately 0.3 ^{o}C/km due to the homogenizing effect of mantle(Winter, 2001).

The most important point to note is that geothermal energy is reponsible for temperature of the ground. Table 4-1 also indicate that temperatures below ground are relatively stable compared to the daily and seasonal variations of above ground temperatures.

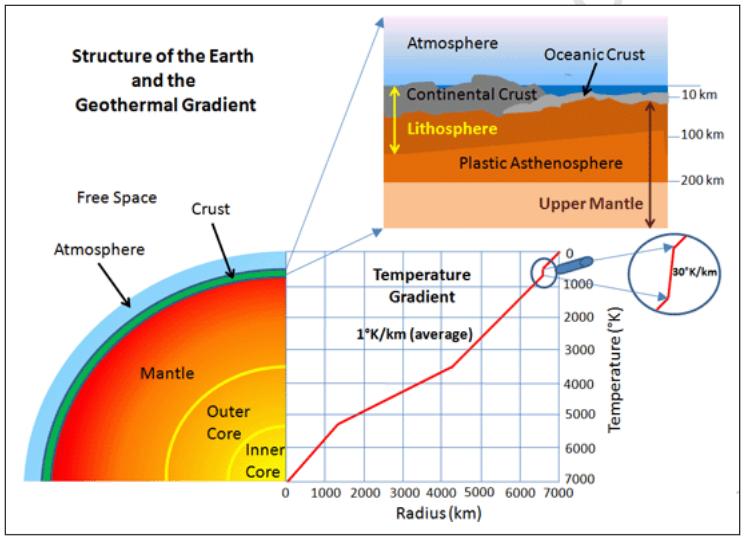

Figure 4-1: Structure of the earth and geothermal gradient (Source: Electropaedia : page on geothermal energy)

Table 4-1: Densities and Temperatures of different earth layers

Layer	Distance from surface (km)	Rock/material composition	Thickness (km)	Density, ρ (g/cm^3)	Temperature (°C)
Crust (continental)	0	Alumino-silicates	70	2.7	varies
Upper mantle	10-300	Iron and magnesium	290	3.4-4.3	1400- 3000
Lower mantle	300-2890	Silicon and magnesium	2600	4.3-5.4	3000 (average)
Outer core	2890-5150	Iron and nickel	2300	10- 12.3	4000-5000
Inner core	5150-6370	Iron and Nickel	1200	15	5000-6000

4.2.2 Variable atmospheric temperatures

Although the Earth's response to the energy balance at the surface is related to the surface air temperature (Geiger,1965), the temperature of the ground continuously includes a response not only to air temperature variations, but also to vegetation, soil moisture variations and solar radiation changes at and near the ground surface. The interaction of all these variables over short or long time scales determines the temperature of the ground.

The variation in surface temperature induced by climate change can penetrate below the Earth's surface and produce an oscillation in the geothermal gradient with periods varying from daily to yearly with amplitude which decreases with depth (Sleep and Kazuya, 1997; Stacey, 1977). For example, daily and yearly temperature variations penetrate into the ground to depths of approximately 1 and 20m respectively (Beltrami and Kellman, 2003) depending on the thermal properties of the subsurface as shown in Figure (4-2).

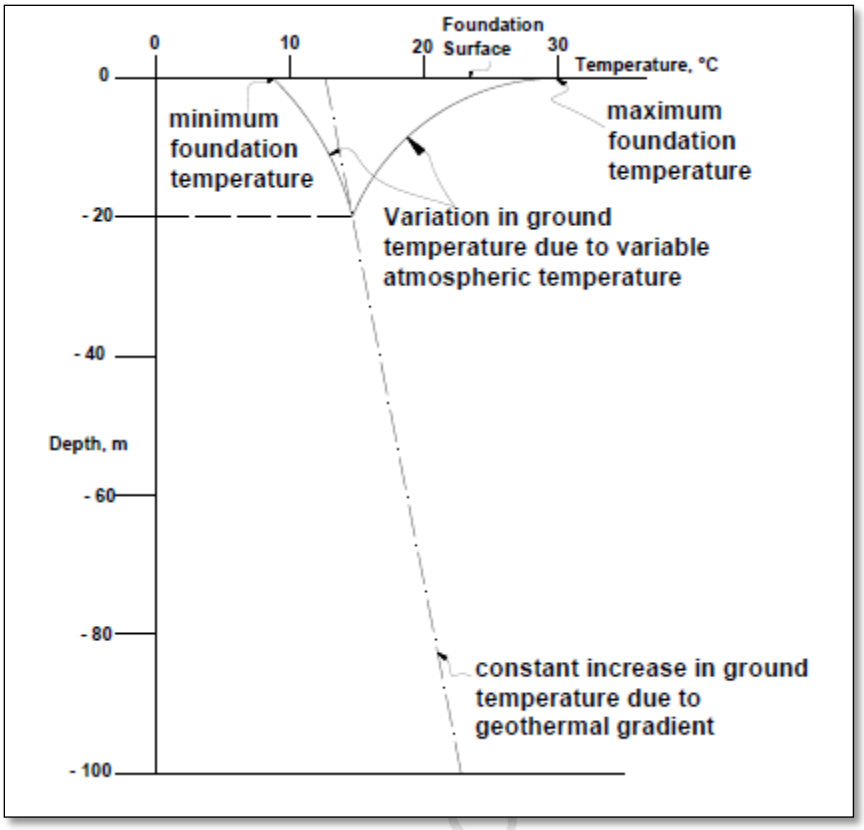

Figure 4-2: Foundation temperature profile

4.3 Dam-Foundation interaction

The most important point of concern to a dam engineer is how the temperature at the dam-foundation interface will influence the temperature distribution in the dam wall. Heat exchange takes place between the dam and the foundation and as such, a part of the foundation should be included in the finite element analysis. But this in some cases has been ignored by researchers. If at all the foundation is included in the model then a simple adiabatic boundary condition is adopted as in equation (4.1) in other cases;

$$\kappa \frac{\partial T}{\partial n} = 0 \qquad [4.1]$$

Where T is the temperature, $\frac{\partial}{\partial n}$ is the normal gradient and k the heat conductivity coefficient. This simplification ignores the heat exchange along the dam-foundation boundary and

therefore causes some errors in this region. However some studies have assumed that heat transfer at the concrete-rock interface occurs only by conduction and the adopted boundary condition is simplified by precribing an imposed constant temperature at the interface. Ardito et al. 2008 pointed out that by assuming a zero thermal flux means unidirectional flow which is not realistic given the large size of the dam hence the latter is considered appropriate. The condition of constant temperature might be considered appropriate but it is inaccurate assumption given the fact the foundation temperature also follow a cylic seasonal variations just like air and water temperature. In this respect, we propose a model that has been applied in establishing the temperature of the ground by Geotechnical engineers to predict the temperature of the dam foundation.

4.4 Proposed foundation temperature model

The analysis of ground temperature by Geotechnical engineers is usually based on the assumption that the temperature variation at the ground surface takes the form of a sine-wave or a Fourier series. This concept has been adopted and used by many authors such as Khatry et al. 1978, Sodha et al. 1979, Krarti et al. 1995, Mihalakakou et al. 1996, Jacovides et al. 1996 and El-Din Salah, 1996 ;1999.

El-Din (1999) stated that the heat flow in the ground usually is expressed by 1-D heat conduction model as

$$\frac{\partial^2 T_g}{\partial z^2} = \frac{1}{D_m}\frac{\partial T_g}{\partial t} \qquad [4.2]$$

Considering the ground as a homogeneous solid with constant thermal properties, the equation (4.2) can be solved with known boundary condition at the ground surface. The energy balance equation (4.2) at the ground surface is therefore used as the boundary condition at the ground surface

$$-\kappa\left(\frac{\partial T_g}{\partial z}\right)_{z=0} = h_c\left(T_a - T_s\right) + a_g\overline{H} - e_g\Delta R - LE \qquad [4.3]$$

Where

T_g = ground temperature; h_c = convective heat transfer coefficient; T_{atm} = atmospheric temperature; T_s = ground surface temperature; a_g = ground surface absorptivity of solar radiation; $\bar{H}$ = solar radiation intensity; e_g = long-wave emissivity of the ground surface; ΔR = difference between the long-wave radiation incident on the surface from the sky and surroundings and the radiation emitted by the black body at air temperature; z = depth; D_m = material thermal diffusivity; k = thermal conductivity of the ground; *LE* is the latent heat flux from the ground surface due to evaporation and given by

$$LE = 0.0168 f h \left[b_1 (1 - r) - b_2 (r_h T_a - T_s) \right] \qquad [4.4]$$

Where *f* is the fraction of evaporation which depends mainly on the ground cover and moisture content of the ground for example, for an arid ground, $f = 0.1 - 0.2$; r_h is relative humidity of the air above the ground surface. For 263 K $\leq$ T $\leq$ 303 K, $b_2 = 103$ Pa K^{-1} and $b_1 = 609$ Pa K^{-1}

Equation (4.3) is rearranged and written as

$$-\kappa \left(\frac{\partial T_g}{\partial z} \right)_{z=0} = h_c \left(T_{amb} - T_s \right) \qquad [4.5]$$

Where; T_{amb} is the ambient temperature due to air temperature T_a and contribution from solar radiation (for the case when $f = 0$)

$$T_{amb} = T_a + \left(\frac{a\bar{H}}{h_c} \right) - \left(\frac{e_g \Delta R}{h_c} \right) \qquad [4.6]$$

The solution to Eq. (4.2) is expressed in sinusoidal form as

$$T_g(z,t) = \bar{T}_0 + A_m e^{-\alpha_o z} \sin(\quad - \quad _o + \quad) \qquad [4.7]$$

Where; $\alpha_o = \left[\frac{\omega}{2D_m} \right]^{1/2}$, $\omega = \frac{2\pi}{P}$, P = period of the cycle, ω = angular frequency

The Eq. (4.6) can also be expressed in sinusoidal form as

$$T_{amb} = \bar{T}_{amb} + A \sin(\quad + \quad _1) \qquad [4.8]$$

$\omega t = \pi/2 - \quad _{max}$, t_{max} is time of occurence of maximum temperature

Substituting from Eqs (4.7) and (4.8) into equation (4.5) gives

$$T_0 = \overline{T}_{amb} \qquad [4.9]$$

$$A_m = A\left[(1+\mu)^2 + \mu^2\right]^{-1/2} \qquad [4.10]$$

and

$$\lambda = \tan^{-1}\left[\frac{(1+\mu)\tan c_1 - \mu}{(1+\mu) + \mu\tan c_1}\right] \qquad [4.11]$$

$$\mu = \frac{\alpha_o \kappa}{h_c}$$

The depth at which the temperature fluctuations are damped can be expressed mathematically as

$$\left|\frac{T_g(\overline{Z},t) - \overline{T}_{amb}}{\overline{T}_{amb}}\right| < \gamma \qquad [4.12]$$

Where $\overline{Z}$ is the damping depth and γ is the small increment ($\gamma = 0.001$)

4.5 Summary

The temperature of dam foundation is affected by two major factors these are geothermal gradient and atmosphereic temperature. Geothermal heat is responsible for the temperature of the ground. The heat flows from inner core of the earth to the earth crust where it is neutralized by the atmospheric effect at the earth's surface. The temperature increase from the earth's surface to the ground is approximated at 3 °C for every 100 m depth.

The variable changes in the earth's surface temperature induced by seasonal changes in weather can penetrate below the Earth's surface and produce an oscillation in the geothermal gradient to a depth of 1 m and 20 m on a daily and annual basis respectively. This variation is howvere dependent on the thermal properties of the subsurface. This means annally, the dam foundation temperature varies relatively to a depth of 20 m after which a relatively constant increase in ground temperature is observed owing to geothermal gradient.

This therfore neccessitates an investigation of how much effect these variable changes in the foundation temperature would have on the entire temperature distribution of dam wall. In order to carry out this investigation, foundation temperature measurements are required. However in the absence the absence measured records, the mathematical model proposed in Eq. (4.7) can ably be used to predict the foundation temperature and it changes with depth. The procedure to perform this investigation is presented in detail in chapter five through finite element analysis taking inot account all the environmental parameters that influence dam temperature.

CHAPTER FIVE

5 FEM IMPLEMENTATION OF PROPOSED FOUNDATION MODEL

5.1 Introduction

The proposed foundation temperature model is implemented in a hypothetical finite element dam-foundation model. Heat transfer analysis is performed considering the effect of air, water, solar radiation as well as foundation temperature.

5.2 Finite element model of dam-foundation system

An accurate finite element model is crucial for any structure analysis. The interaction effects between the concrete wall, its foundation, impounded reservoir and ambient air have to be taken into consideration in order to understand the structural response.

The process of building a finite element model requires that such parameters as loads applied to the structure, boundary conditions and material properties are all chosen correctly

5.2.1 Finite element idealization of dam-foundation system

The underlying principle behind finite element method is that a physical structure is modelled as an assemblage of individual elements connected at their nodes. The arch dam is idealized as an assemblage of two parts (ie wall and its rock foundation) acting as a single structure rigidly connected together at their interface.

ABAQUS, a commercially available general purpose finite element package has been used for developing the model. ABAQUS has been preferred in this case due its several advantages over other solvers in relation to thermal analysis of concrete dams. These include the ability to model heat transfer across the thickness with high accuracy and ability to simulate dam-foundation interaction well (Labibzadeh et al. 2010).

5.2.2 Finite element idealization of concrete wall and its rock foundation

The dam wall is modeled as structure with the upstream face completely covered with water and the entire downstream face including the crest exposed to air. A typical dam wall with a height of 90 m has been modeled. It is modeled as 3-D deformable homogenous solid concrete

section. The wall has been partitioned into three sections over the height (i.e bottom, middle and top) to compute the concrete average temperature such that the variations in thermal response at different locations are clearly observed. Additionally it was partitioned in this way to aid in the meshing of the critical sections of the model where the structure is very responsive to load changes and also to facilitate in applying the loads and boundary conditions.

On the other hand, in a typical finite element model the rock foundation is normally discretized as a rigid homogeneous structure with the depth below the foundation kept equal to the height of the dam and width of the foundation equal three times the width of the dam at foundation level (Arya et al. 1995). The large volume of the rock foundation is usually included in the dam model to be able to adequately capture the foundation boundary condition and its effect on the thermo-mechanical response of the dam (Nissar et al. 2008).But for the purpose of this investigation, the rock foundation is simplified as rectangular and modeled as 3-D homogenous solid rock section with a depth of 60 m. Figure (5-3) shows the hypothetical 3-D finite element model of the dam-foundation system

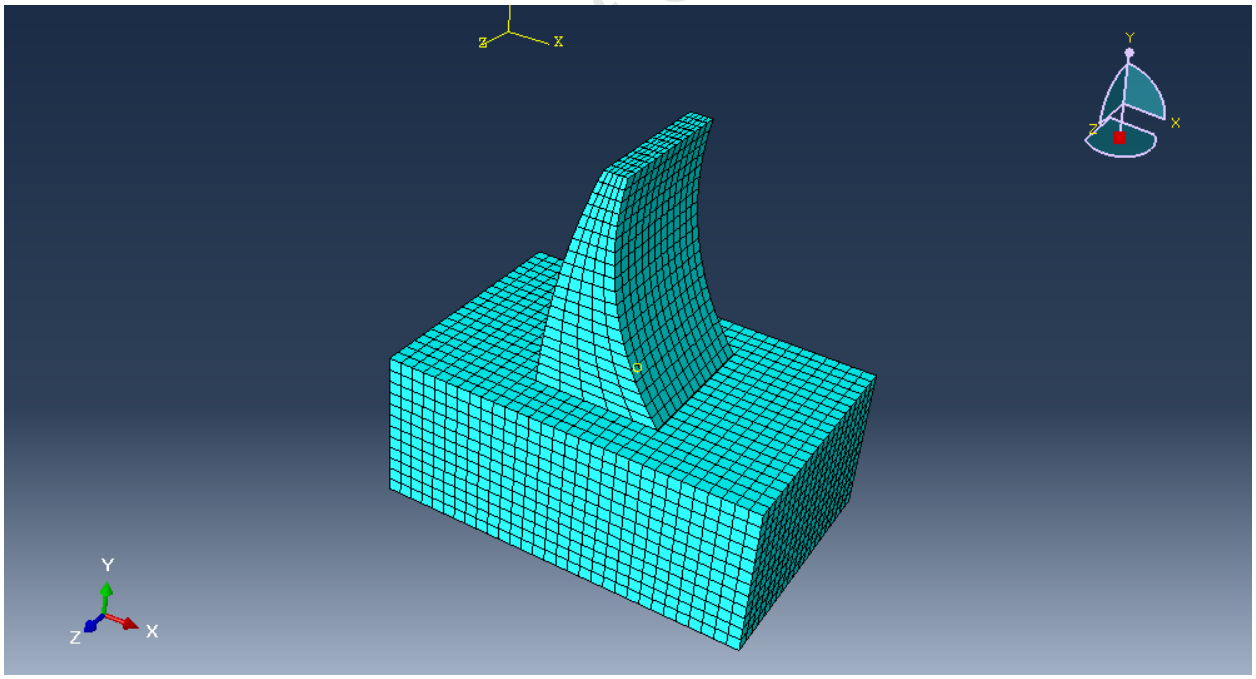

Figure 5-1: 3-D finite element model of the dam-foundation system

5.3 Thermal analysis algorithm in ABAQUS

In thermal analysis, thermal loads in the form of heat fluxes and temperatures are applied in every step. Between the time intervals, the program calculates the average values of the thermal load. A typical finite element analysis procedure is given in Figure (5-1).

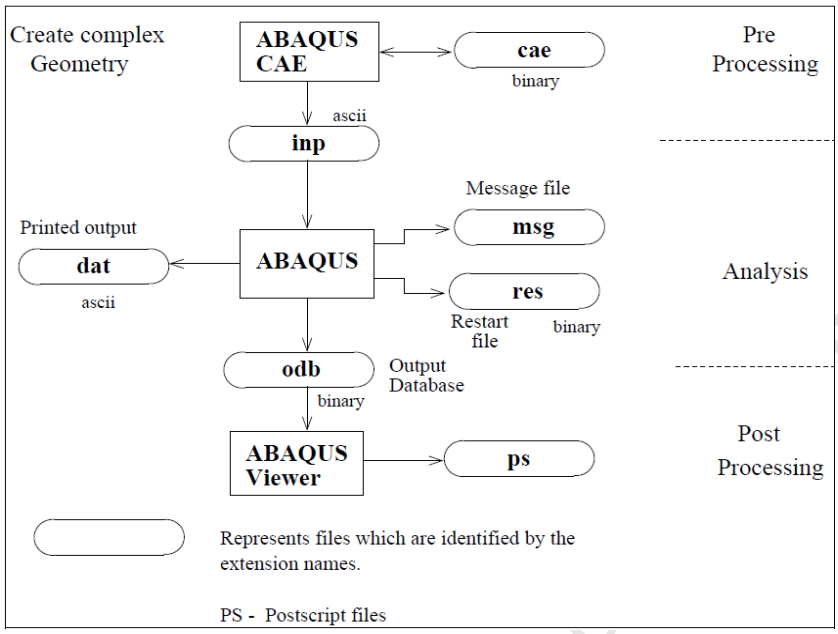

Figure 5-2: FEA using ABAQUS

The incremental thermal analysis algorithm is presented in the flow chart in Figure (5-2). This is the easiest way to present the sequence behind the simulation techniques.

In the algorithm, the first step presents preprocessing stage in which the user creats the geometry, defines material properties associated with it, analysis steps, element types, any interactions of any contact surfaces, apply boundary conditions and loads and finally mesh the geometry.

Analysis type: 3-dimensional heat transfer analysis and this calculates the thermal quantities of the model. The most important thermal quantities of interest are the temperature field, thermal flux and thermal gradient.

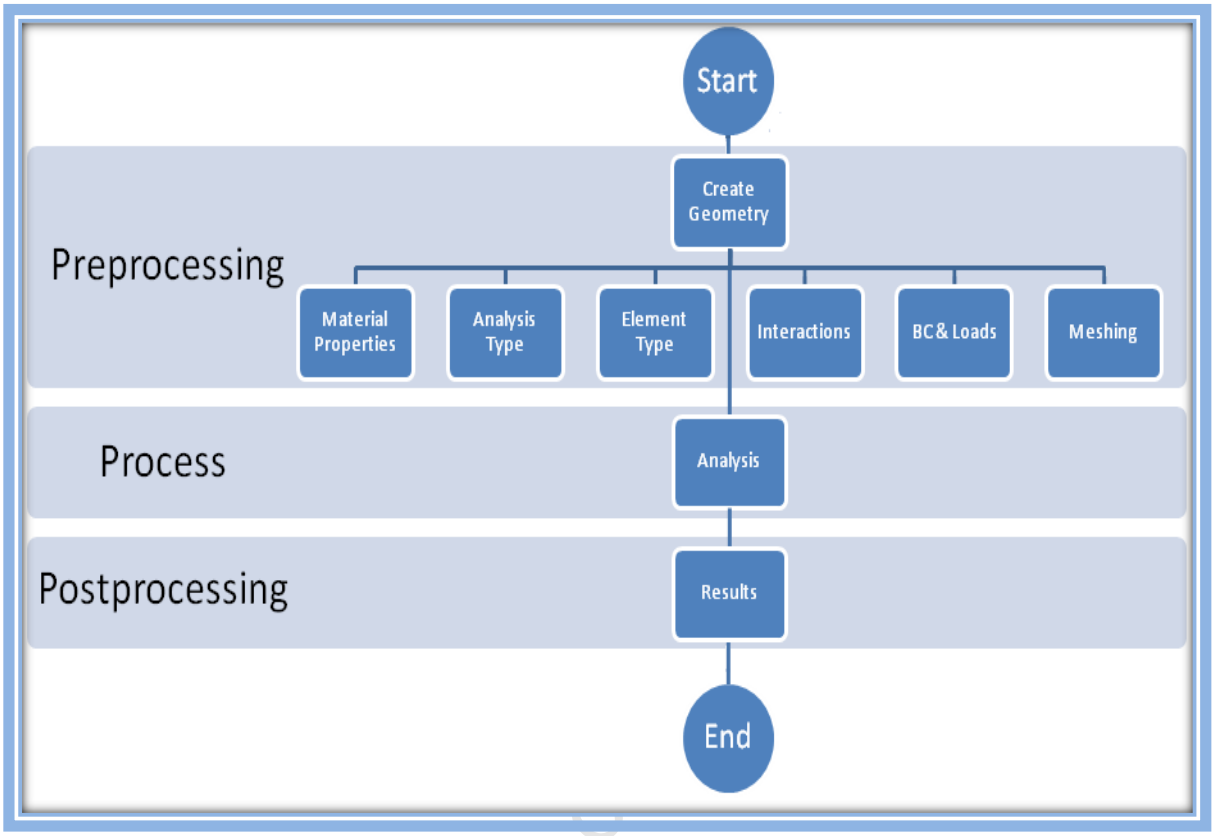

Figure 5-3: Finite element modeling algorithm for themal analysis

Element type: 3-D linear solid heat transfer elements have been selected. 8-node linear hexahedron brick element (DC3D8) have been used for both the foundation and concrete wall.

Material properties: thermal and mechanical properties of rock foundation and concrete wall required for the analysis are thermal conductivity k, density ρ, specific heat, c, and heat coefficients (for concrete) and dimensionless constants for the analysis are given in the Table 5-1.

Table 5-1: Thermal and mechanical properties

Property	Units (SI)	Concrete	Rock
Thermal Properties			
Thermal conductivity, *k*	W/(m.K)	2.5	2.2
Specific heat, *C*	J/(kg.K)	900	840
Solar absorptivity, *a*		0.65	n/a
Emissivity, *e*		0.9	n/a
Mechanical properties			
Density, ρ	Kg/m^3	2400	2400

Boundary condition and load parameters: This will include surface fluxes, surface films, surface radiations, boundary specified temperatures

After preprocessing , the load step is submitted for the solution of the temperature field at every node. This is the processing stage done by the computer

Finally the last step is the postprocessing where temperature time history are obtained for the whole model.

5.4 Heat transfer analysis

Abaqus is capable of performing linear and nonlinear steady-state and transient heat transfer analysis. In the steady-state analysis it is assumed that the temperature response of the dam does not vary with time. This means that the temperature at every point within the dam wall including the surface is independent of time. Transient thermal analysis meanwhile determines the temperature distribution and other thermal quantities under temperature conditions that vary over time, in which case the loads are prescribed as functions of time. In a nonlinear analysis, the solution cannot be calculated by solving a single system of linear equations (the finite element equations in Chapter 2), as would be done in a linear case. Instead, the solution is found by specifying the loading as a function of time and incrementing time to obtain the nonlinear response. Therefore, ABAQUS breaks the simulation into a number of time increments and finds the approximate equilibrium configuration at the end of each time

increment. Using the Newton method, several iterations are done to determine an acceptable solution to each time increment. The procedures discussed in Chapter two,section 2.4 has been adopted in this study.

5.4.1 Assumptions adopted in the analysis

For the purpose of temperature distribution analysis of concrete dams in operation, the temperature of concrete varies in relatively a small range of 255-310 K (Leger et al. 1993a) and the temperature dependence on thermal and mechanical properties of concrete are considered negligible that is the conductivity of concrete is assumed isotropic. In this period also,the heat transfer process is not affected by the latent heat effects during phase change. Therefore the mechanical and thermal properties of concrete are assumed constant, isotropic and temperature independent and the phase change phenomena is ignored.

Heat of hydration has been completed and hence the internal heat generation is neglected

At concrete-water interface, it is assumed that convection and radiation do not occur at the interface. Thus the concrete temperature incontact with water is equal to water temperature

At dam-foundation interface the only heat tranfer mechanism taking place is conduction with the assumption that no water flows through the interface

5.5 Treatment of boundary and initial conditions in the model

Thermal response of the model is driven by thermal loading through prescribed temperatures, surface fluxes, heat transfer coefficients and surface radiations. The Figure (2-5) has been adopted to implement the heat transfer processes and the boundary conditions in this study

5.5.1 Concrete-Air interface

The boundary conditions considered are heat flow from the sun (solar energy), convection between the concrete surface and ambient, and radiation from concrete surface to the ambient.

Air temperatures

As there were no direct site measurements for air temperatures, the Eq. (3.22) was used to approximate the daily air temperature records to input in the finite element model. The daily temperature records for Cape Town was obtained from South African Weather Service, and

typical design year of 365days was established. The records cover a period of 14 years from 1995 to 2009. The daily and monthly design air temperatures were obtained by averaging the recorded temperatures. Figure (5-4) shows the average daily and monthly design air temperatures. The minimum average daily air temperature of 7 °C occurs in July, while the maximum average daily air temperature of 26° C occurs in January and February.

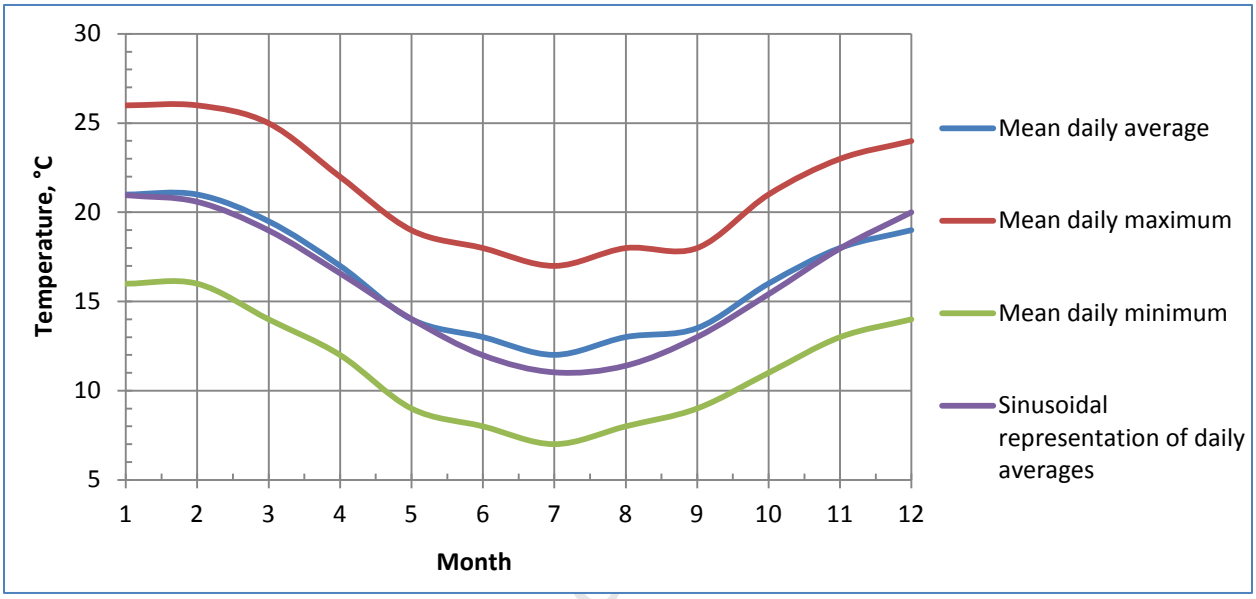

Figure 5-4: The average daily and the monthly design air temperatures

Heat transfer coefficients

The Equation (3.20) was adopted to define the convective heat tranfer at this interface. The convective heat coeficient was obtained using Equation (3.21c) using the annual average wind speed of 3.42 m/s for Cape Town shown in Table (5-2)

Table 5-2: wind speed records in Cape Town

Month	Jan	Feb	Mar	Apr	May	June	July	Aug	Sept	Oct	Nov	Dec
Avg Wind Speed(m/s)	4	4	3	3	3	3	3	3	3	4	4	4

Surface radiation to ambient

The Equation (3.17) was adopted and modified as per the software requirement as given below

$$q_r = h_r\left[\left(T_s - T_z\right)^4 - \left(T_a - T_z\right)^4\right] \qquad [4\text{-}4]$$

T_z is the value (i.e. 0 °C 0r 273 K) of absolute zero , h_r is the radiation constant defined as

$$h_r = e_c C_s \qquad [4\text{-}5]$$

Where: e_c is the emissivity of the concrete surface and C_s is the Stefan-Boltzmann constant

Incident solar radiation on the concrete surface

To obtain the total amount of solar energy, $\bar{H}$, reaching the concrete surface, the Eq. (3.1) was adopted. Based on results published by Power and Mills (2005), see Appendix A, the monthly average of quantity $\bar{H}$ was obtained considering the effect of direct, diffuse and reflected solar radiation components in Eq. (3.15). This quantity was also considered variable in time and Equation (3.22) was used to define its time variation in the finite element model

5.5.2 Concrete-Water interface

The proposed model by Bofang and Zhammei (1990) in Eq. (3.24) has been adopted here to approximate the water temperature. Due to lack of data for reservoir temperature history, it was assumed initially that the reservoir surface assumes the temperature of the ambient. Based on this guess, this value was extrapolated to a depth of 20 m. Below this depth, the reservoir temperature was assumed to attain the annual average. Based on information obtained, the annual average temperature of natural reservoir in Western Cape lies between 10 °C and 14 °C, hence 12 °C was used to represent the annual average reservoir temperature in the model.

5.5.3 Dam-Foundation interface

Daily and annual fluctuations in foundation temperature are mainly affected by variations in the air temperature, solar radiation (i.e. exposed portion) and water temperature (i.e. portion

beneath the reservoir). The proposed model in Equation (4.6) is now used to predict the periodic variations of ground temperature with time and depth.

Due to lack of measured data for foundation temperature, 2°C was added to air temperature on the exposed ground surface to account for the contribution from solar radiation, the foundation temperature beneath the reservoir was assumed to have the same temperature as that of the reservoir and the temeprature of the foundation portion underneath the wall was obtained as the average between the exposed portion and portion beneath the reservoir.

5.5.4 Initial condition

To start the transient computations, a steady-state heat transfer analysis was done by applying mean annual air and water temperature at the concrete-air and concrete-water interface respectively. The mean annual air temperature was increased by 2 °C to account for solar radiation effect. At the dam-foundation interface annual average temperature for three portions of the foundation were prescibed. The heat tranfer results and corresponding thermal stresses are presented in Chapter six.

5.6 Parametric investigation

The air, reservoir, and foundation temperatures as well as solar radiation have been previously described. There are always uncertainties associated with evironmental parameters. The uncertainties are due to the variability of climatic conditions from year to year, and lack knowledge of the temporal and spatial distribution of temperature and heat fluxes at the boundaries of the dam. Therefore, a parametric study is conducted to assess the influence of variable foundation temperature and variable water level. The effect of solar radiation and air temperature have been dealt with by Sheibany and Ghamiean (2006) and Leger et al. (1993b) respectively.

5.6.1 Effect of reservoir temperature and variable water level

The reservoir surface temperature is approximately equal to the air temperature. Three different cases have been selected for this investigation.

Case 1: Full reservoir capacity: This is when the whole upstream face of the dam is assumed to be covered with water. This was assumed to be associated with with wet and extreme cold conditions hence the wettest was year selected for the investigation

Case 2: Half-full reservoir: This is based on the assumption that the reservoir remained half-full for most part of the year. The average temperature used in case 1 and case 3 was applied in this case

Case 3: Low level reservoir (1/4 of dam height): This is when most part of the upstream is left exposed to air and solar radition. This was assumed to be associated with dry and hot conditons for a given year hence the warmest year was used. The results to this investigation are presented in Chapter six

5.6.2 Effect of variable foundation surface temperature

As opposed to applying a uniform constant foundation temperature and assuming adiabatic condition at the dam-foundation interface, three partitions of the foundation have been considered to investigate the effect of spatial and temporal variability of foundation temperature i.e. the exposed surface, portion underneath the wall and portion beneath the reservoir. Each section is specified with temperature of a certain magnitude which varies with depth and time. Two years in which highest and lowest air temperature were recorded have been used carry out the investigations. These values were chosen to simulate extreme conditions experienced by the dam. Prescribed uniform constant foundation temperature are compared with prescibed spatially time varying foundation surface temperature and results are presented in Chapter six

CHAPTER SIX

6 RESULTS, ANALYSIS AND DISCUSSION

6.1 Convergence of Heat Transfer Analysis

The concrete wall was divided into three sections. Figure 6.1 shows the time history of the average temperatures for the concrete wall including top, mid and bottom sections using a time step of one day. Convergence, which is obtained for the second year of analysis, is defined when the average concrete temperature evaluated on January first varied by no more than 1 % for top,mid and bottom sections. If, as a convergence criterion, the temperature of a node located at the centre of each section is considered, convergence is achieved on the third year. Therefore 365 daily temperature distributions for the third year of analysis were chosen to represent the typical average temperature of the concrete wall due to seasonal temperature variations.

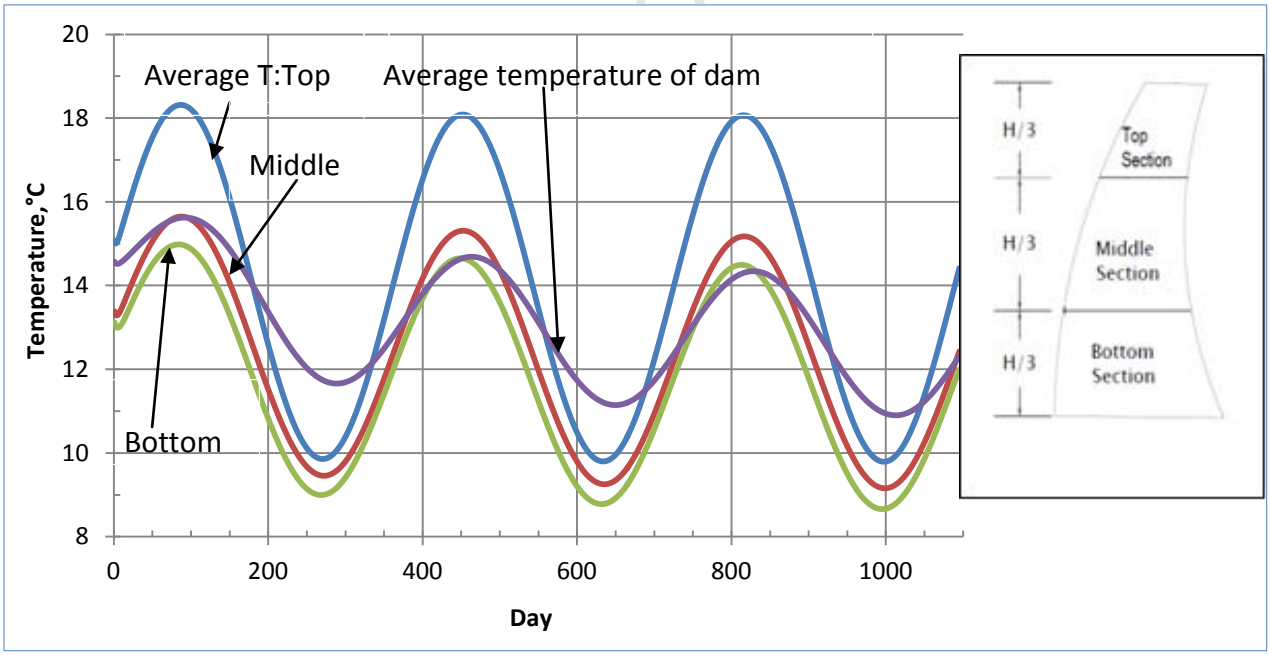

Figure 6-1: Convergence of the numerical solution

6.2 Transient thermal response of the concrete wall

Following convergence of the thermal analysis, 365 daily temperature distributions that were assumed to be a good representation of a typical yearly response of the concrete wall were obtained. Figure (6-2) shows the time history of the average temperatures of the dam top, mid and bottom sections due to seasonal variations of air, reservoir, foundation and solar radiation. A time lag of 35 days is observed between the time at which the maximum average temperature of the concrete is reached and the time at which the maximum air temperature occurs. The annual average temperature for the concrete wall was computed as 12.63 °C with annual air temperature of 15 °C

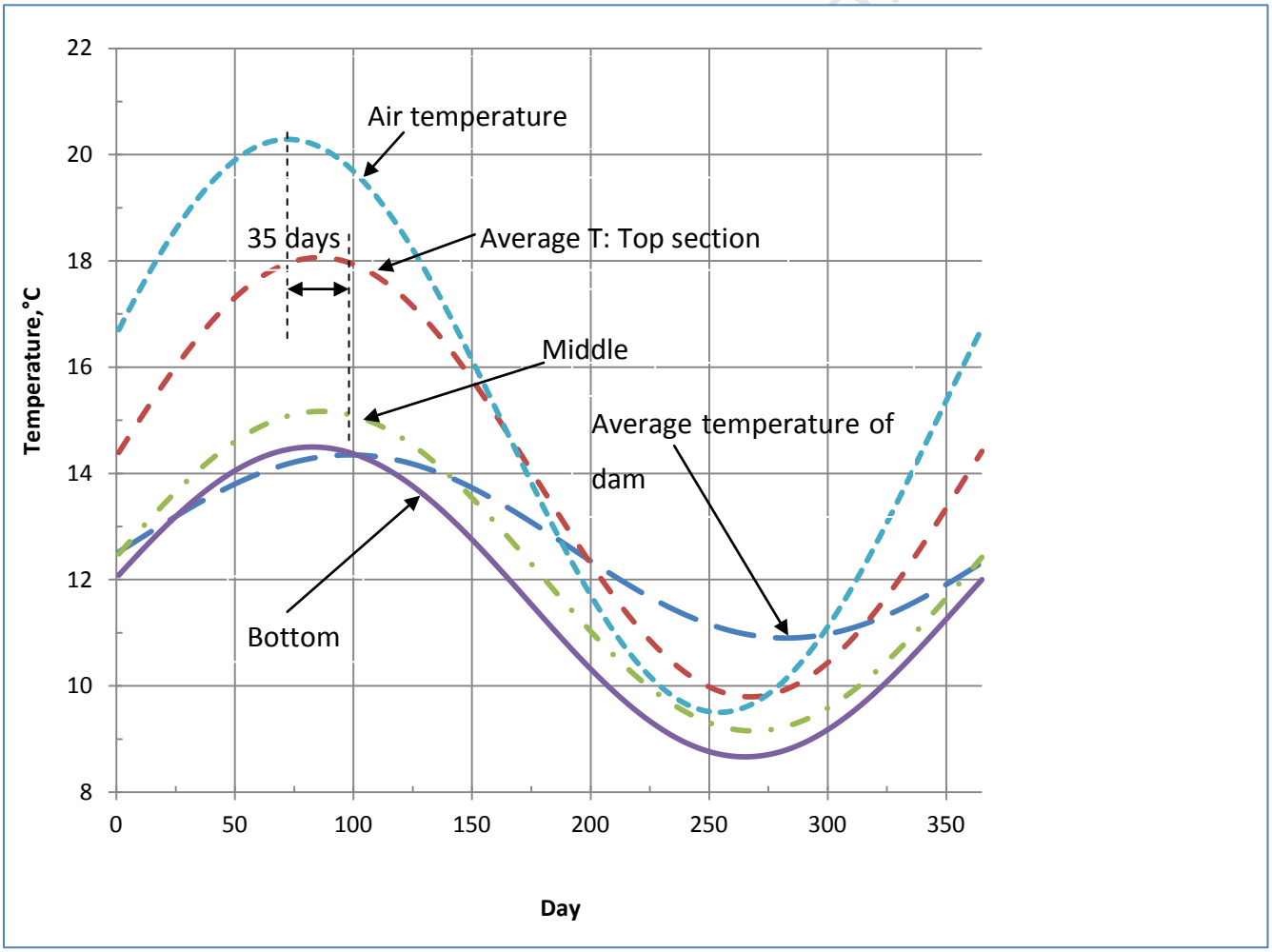

Figure 6-2: Average thermal response of concrete

6.3 Annual temperature and stress distributions in the dam

To study the temperature and stress distributions in the dam, daily temperature distributions were used to carryout the 365 stress analysis. Figures 6-3a shows the temperature distributions contours for the day when maximum air temperature (at day 80) was reached. High thermal gradients are observed along the downstream face including the crest exposed to air and solar radiation over a depth of approximately 3 m. The maximum temperature of approximately 22 °C is recorded near the crest edge of the dam. Figure 6-3b presents the maximum principal stress contours corresponding to temperature distributions computed from heat transfer analysis shown in 6-3a. High maximum principal stresses corresponding to these temperature distributions are observed at the edges of the crest and near the heel and toe of the dam model. The highest value of tensile stress recorded is 1.82 MPa near crest.

Figures 6-3c presents temperature distributions when minimum air temperature is recorded (on day 196). On this day, maximum concrete temperature of about 18 °C is recorded approximately 4 m from the downstream face of the dam. This result is expected due to thermal inertia of the concrete in responding to the air temperature variations. Figure 6-3d corresponds to stress contours for the temperature distributions shown in 6-3c. The highest maximum principal stress recorded is 1.26 MPa occurring at an internal node near the crest.

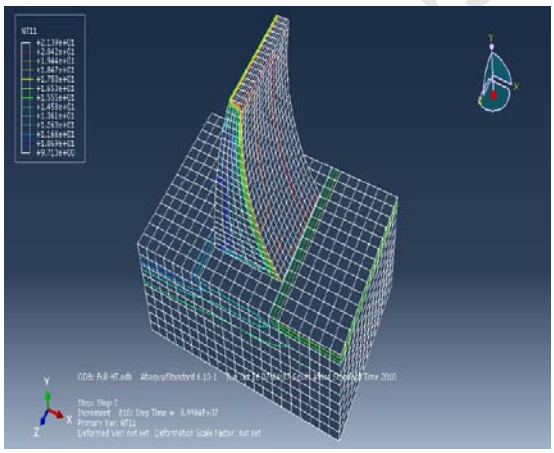

(a)

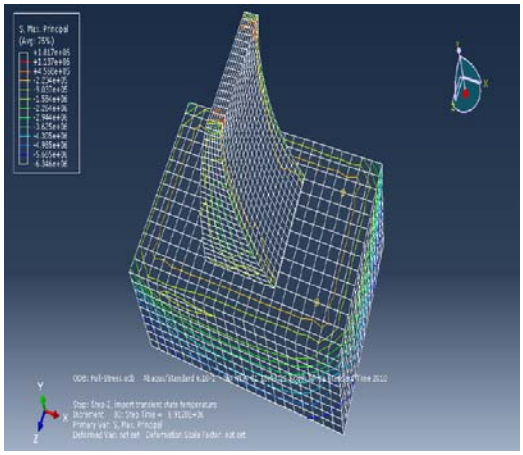

(b)

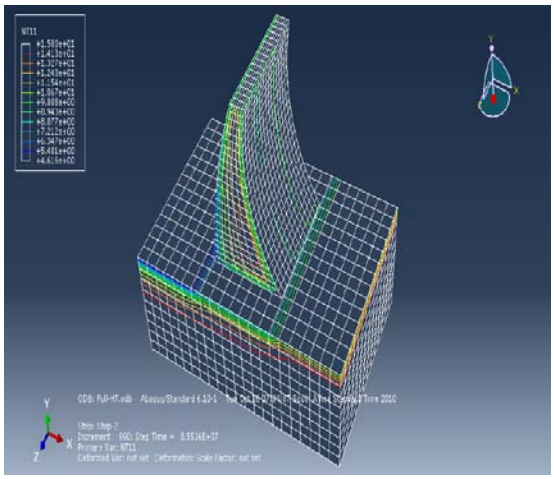

(c)

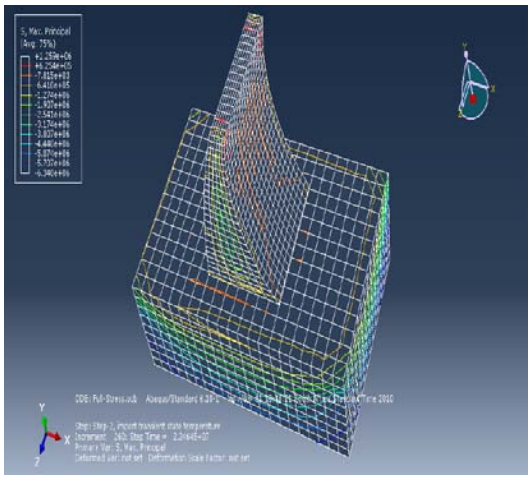

(d)

Figure 6-3: Temperature and Stress contours: (a) day when maximum air temperature occurs; (b) Stress contours corresponding to day of maximum air temperature; (c) day when minimum air temperature occurs; (d) stress contours corresponding to day of minimum air temperature

6.4 Effect of variable foundation surface temperature

As mentioned, the foundation is sometimes not included in finite element transient heat flow analysis. When it is included, adiabatic condition is assumed at the dam-foundation interface. In this study, heat exchange is assumed at the interface through conduction considering variable and constant foundation surface temperature. Figures (6-4) – (6-7) show the thermal response of the dam when a spatially time varying and constant uniform foundation temperature is prescribed. For the year considered marked difference in average temperature at the interface is observed for a set of nodes running longitudinally and transversely through the dam wall. In Figure (6-4a) the temperature of the concrete for the nodes in contact with the foundation is at 18.4 °C when spatially time variable foundation temperature is prescribed compared to 16.1 °C for the when constant foundation temperature is applied in Figure (6-4b). A rapid decrease from 18.4 °C to approximately 16.8 °C in concrete temperature is observed, 10 m from interface when a variable foundation temperature is prescribed (see Figure (6-4a)) compared to a gradual increase from 16.1 °C to 16.8 °C for the same set of nodes when a constant foundation temperature is prescribed (see Fig (6-4b)). It is also observed in Figures (6-4a and 6-4b) that,

30 m from dam-foundation interface, the concrete temperature in both cases is approximately 17 °C. This can be interpreted to signify zone in which variable foundation temperature has negligible influence on the concrete temperature.

For transverse temperature profile across the dam wall shown in Figures (6-5a and 6-5b), the concrete temperature remains approximately constant at 18.4 °C for a node 5 m from dam-foundation-water interface and dam-foundation-air interface for the case in which variable foundation temperature is prescribed compared with the 16°C observed when constant foundation temperature is prescribed in Fig (6-5b). This clearly shows the influence foundation temperature has on the thermal response of the dam at the interface.

A similar discussion as above can be deduced for the condition in which lowest air temperature was recorded as shown in Figures (6-6) and (6-7)

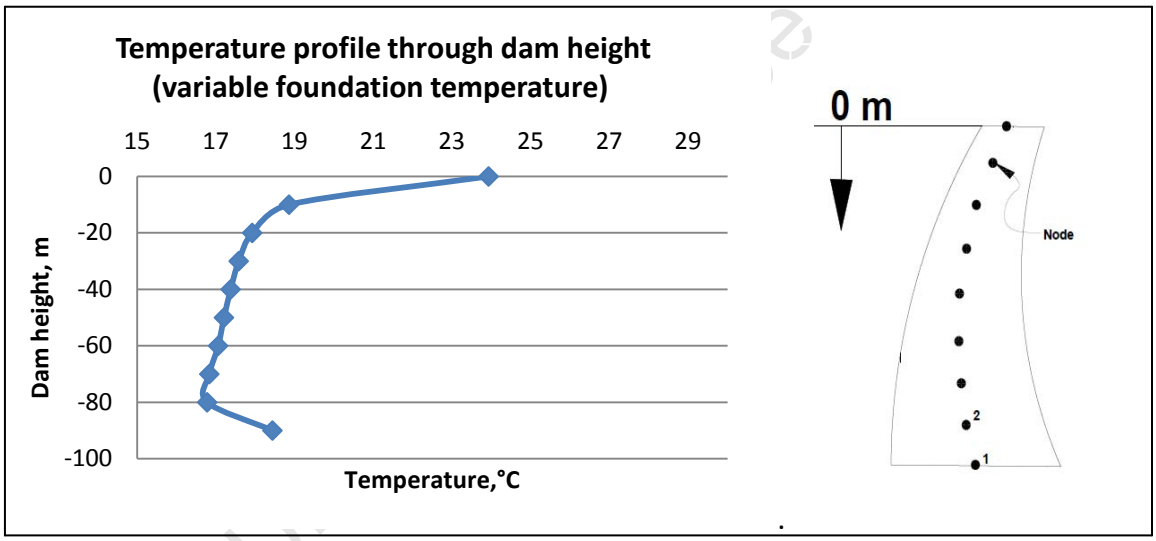

(a) Prescribed variable foundation temperature

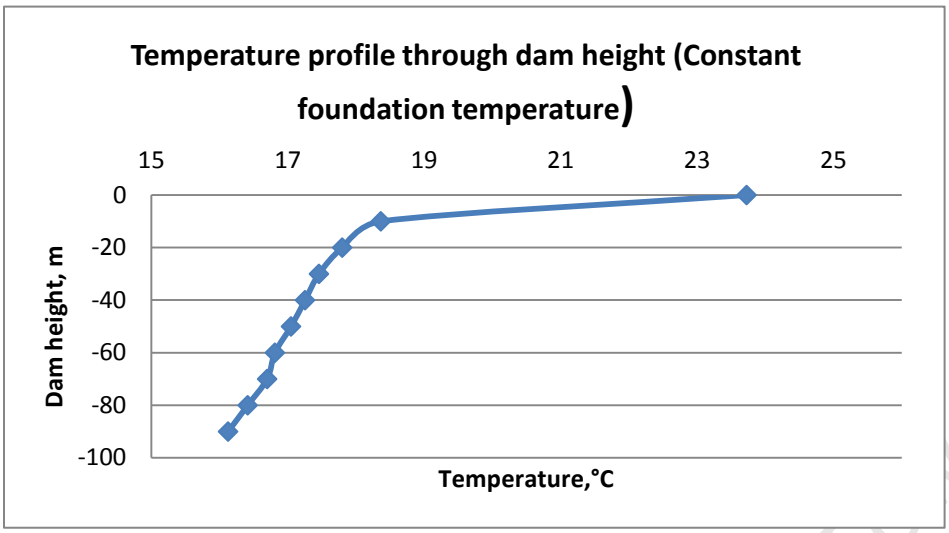

(b) Prescribed constant foundation temperature

Figure 6-4: Longitudinal temperature profile through the dam wall for maximum air temperature

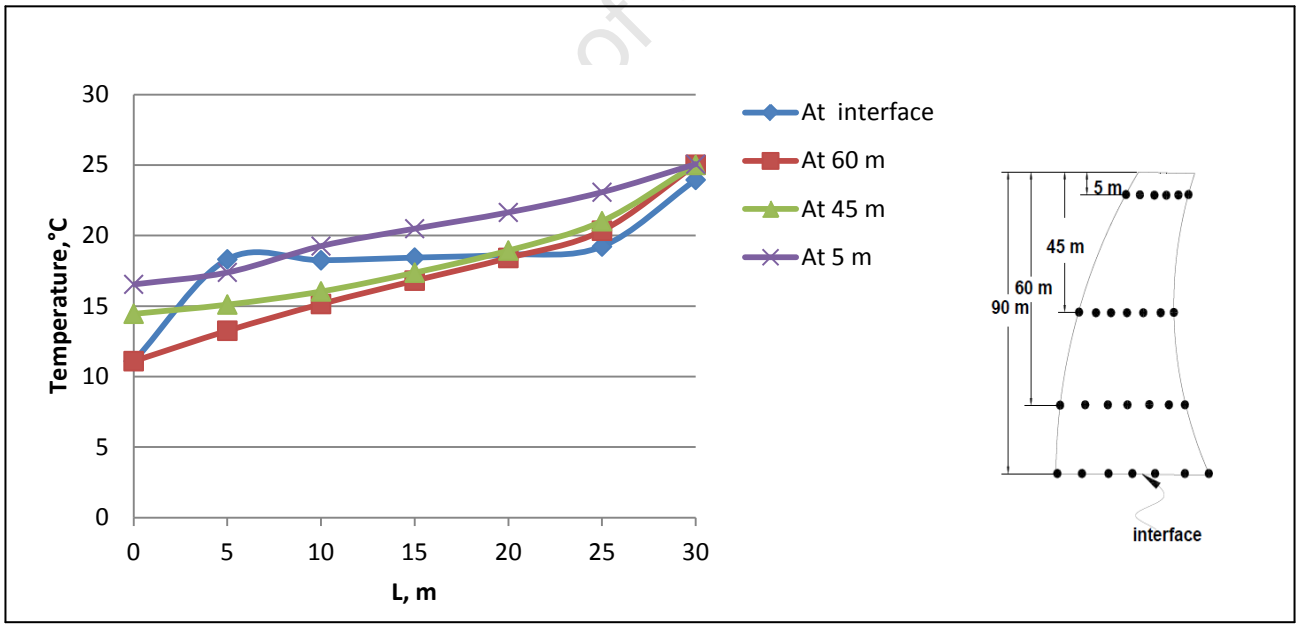

(a) Prescribed variable foundation temperature

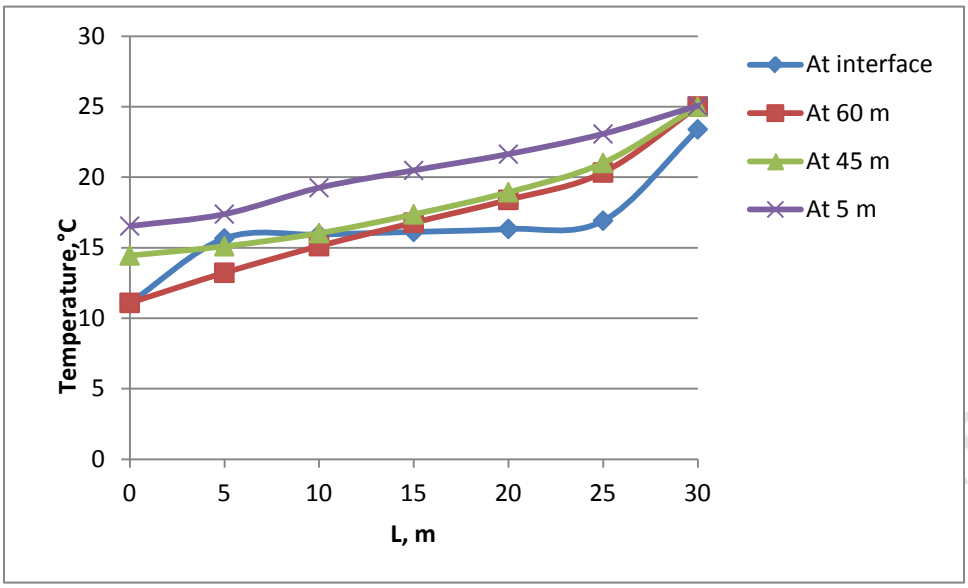

(b) Prescribed constant foundation temperature

Figure 6-5: Transverse temperature profile across the dam wall for maximum air temperature

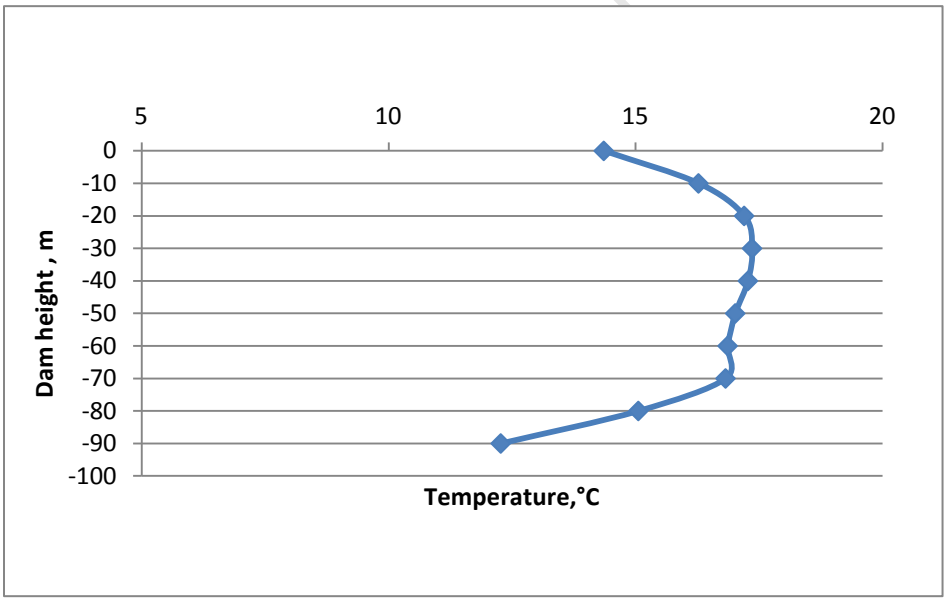

(a) Prescribed variable foundation temperature

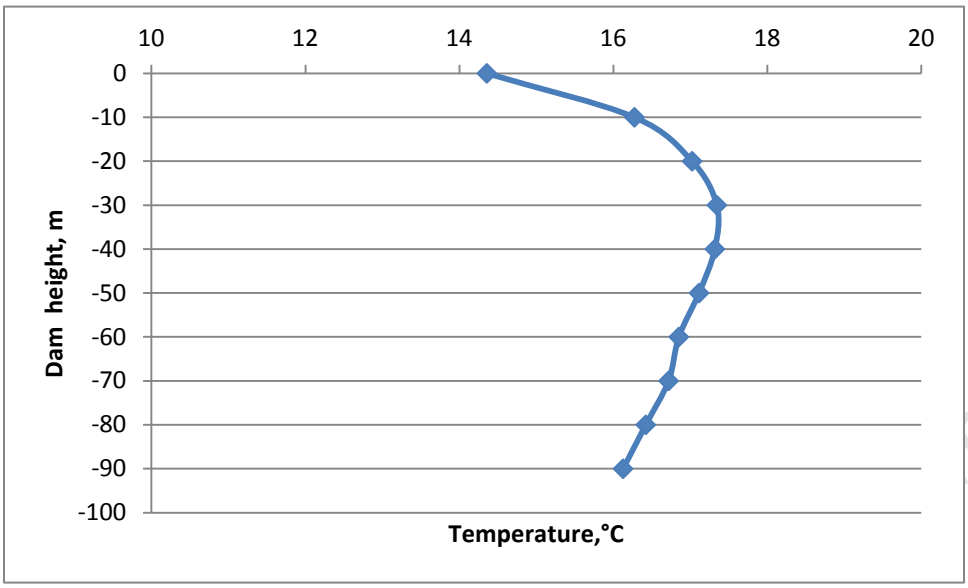

(b) Prescribed constant foundation temperature

Figure 6-6: Longitudinal temperature profile through the wall for minimum air temperature)

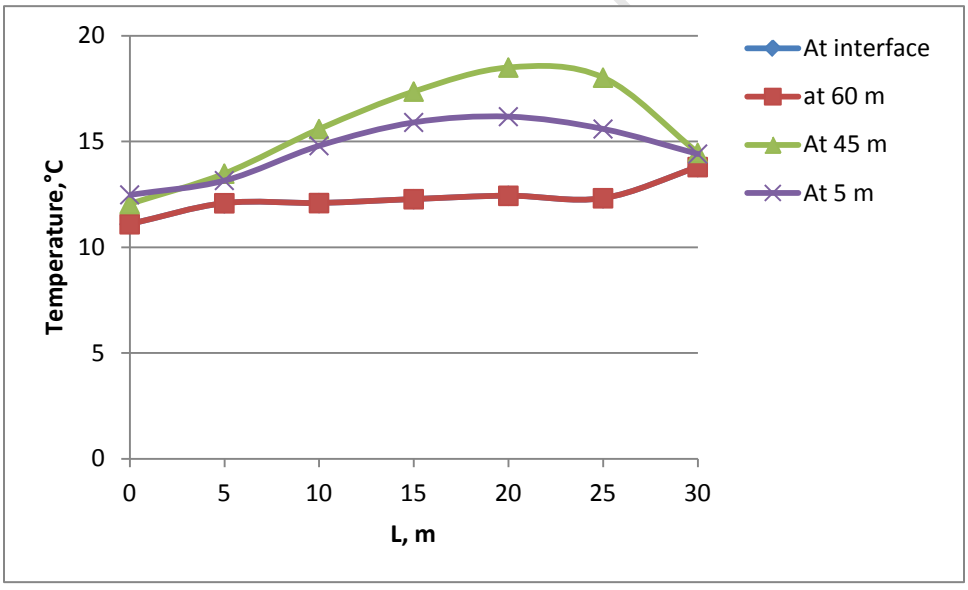

(a) Variable foundation temperature

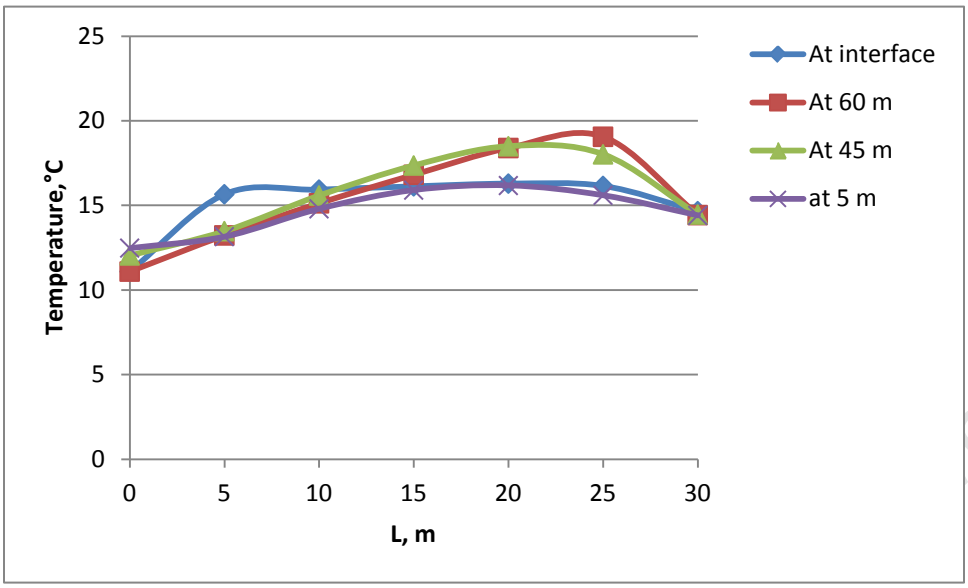

(b) Constant foundation temperature

Figure 6-7: Transverse temperature profile across the wall for minimum air temperature

The effect of variable foundation temperature on thermal stress response of the dam was investigated for two nodes; node 1 located at the dam-foundation interface and node 2 located approximately 7 m from the interface are considered. As shown in Table 6-1, the effect of foundation on thermal response of the dam is significant. When spatially time varying foundation temperature is prescribed, the maximum increase in the nodal temperature is 17.6% and 3% for nodes 1 and 2 respectively. This occurred on day 63 and 172 for node 1 and 2 respectively. These results also indicate the effect is significant at the interface and has very little effect on the response away from the dam-foundation interface. It can be seen from Table 6-1 that the foundation temperature has negligible effect on thermal stress response at the interface for the corresponding temperature distributions computed from the heat transfer analysis. However a 9% increase is observed in the maximum thermal stress obtained at node 2. It should be noted that the day of maximum temperature does not correspond to day of maximum tensile stress for nodes considered

Table 6-1: Influence of foundation temperature on thermal stress response of the dam wall

Case	Max Temperature (°C)		Min Temperature (°C)		Max Tensile Stress (MPa)		Min Tensile Stress (MPa)	
	Node 1	Node 2	Node 1	Node 2	Node 1	Node 2	Node 1	Node 2
Variable	$20.05^{(63)}$	$17.18^{(172)}$	$13.94^{(244)}$	$16.29^{(1)}$	$1.98^{(89)}$	$3.46^{(81)}$	$1.28^{(285)}$	$0.86^{(1)}$
Constant	17	16.72	17	16.63	2.01	3.18	1.27	0.89

(*) day in which results were obtained

6.5 Effect of variable water level

Because the temperature of concrete is influenced by the temperature of the impounded water, to investigate the effect of variable reservoir level on the thermal response of the wall, the annual average concrete temperature have been compared for the three different scenarios under study. The results in Table 6-2 shows that the average concrete temperature is highest when the upstream face is exposed to air and solar for most part of the year and lowest average temperature when reservoir is full. This therefore means that exposure to air temperature and solar radiation on the upstream face increases the concrete average temperature by 53.7 % hence water level on the upstream has significant effect on the overall concrete average temperature

Table 6-2: Effect of variable reservoir water level on concrete temperature

Water level	Concrete Average temperature (°C)
Full	12.63
Half-full	16.69
Low	19.41

Further investigation was carried on two nodes at mid height of the dam; node 3 located on the dam-water interface and node 4 approximately located 0.5 m from the dam-water interface were chosen to investigate the effect of water level to thermal stress response of the dam. Two cases have considered here i.e full reservoir and low reservoir water level. The results in Table 6-3 indicate that high temperature and stresses are recorded for low reservoir level. This further confirms the effect of water level to thermal stress response of the concrete.

Table 6-3: Effect of variable water level on the thermal stress response of the dam

Water Level	Max Temperature (°C)		Min Temperature (°C)		Max Tensile Stress (MPa)		Min Tensile Stress (MPa)	
	Node 3	Node 4	Node 3	Node 4	Node 3	Node 4	Node 3	Node 4
Full	10.00	10.87	6.00	9.47	0.51	0.51	-0.05	-0.05
Low	25.39	20.66	14.48	17.89	0.71	0.71	-0.18	0.18

CHAPTER SEVEN

7 CONCLUSION AND RECOMENDATION

7.1 Summary

This dissertation has provided a detailed literature review on the current state-of-the-art temeprature models for establsihing temperature distribution in existing concrete dams. It then extended further to provide a comprehensive review on the environmental paramaters that affect the temperature distribution for concrete dams in operational stages. After which an investigation is carried out to establish the influence of variable foundation foundation temperature and fluctuating water level on temperature distribution in concrete dam walls.

This Chapter therefore re-examines the results in light of the original thesis and provide basis for claims made in chapter one. It concludes with an exploration of possible future directions for the research

Through an extensive literature review on the temperature models, it was observed that, currently, the Fourier heat conduction equation is the only adopted mathematical model to describe the mechanism of heat flow phenomena in the concrete dam wall. Much as there is only one equation used to explain heat transfer mencahisms in dam wall, several other models to understand the heat transfer mechanisms at the dam boundaries have also been presented such as the convection, radiation models as well conduction models.

A number of numerical techniques have been adopted to obtain the complete solution to the Fourier heat conduction models and to implement other boundary condition models in order to establish the temperature field in the dam. These include meethods such as finite element method (FEM), finite difference method (FDM), finite volume method (FVM) and Fourier series analysis (FSA).

The finite element analysis (FEA) approach besides its limitations such as large computational effort and required expertise, is currently the most preferred approach to the solution of heat

transfer equations. This is particularly due to its ability to deal with irregular geometries and complex boundary conditions and loadings which are the limitations of FDM and FVM.

From the available literature obtained, it is noted that temperature distribution in concrete dams in operation is controlled by seasonal temperature changes and climatic conditions. The seasonal variations in air, reservoir and foundation temperature as well as solar radiation including wind effects are responsible for temperature field in concrete dams in operational stages.

Knowledge of concrete temperature condition is essential for the analysis of thermally induced stresses within the dam structure. Transient changes of the temperature distribution inside the concrete result in significant thermal tensile stresses in the structure. Therefore transient temperature distribution analysis on concrete dams forms the basis of thermally induced stress computations. A reliable thermal analysis method in finitre element technique and computational procedures has been established. The computation problems encountered in the method are the initial and boundary conditions. All the boundary conditions considered are environment dependent which are extremely difficult to implement. An initial temperature field must be assumed to start the transient heat flow analysis. This means that an error is introduced at the beginning of the analysis. Studies have shown that after a certain time, this error decreases to a negligible level in other words the solution converges to a real one.

To investigate the influence of variable foundation temperature and fluctuating water level on concrete dam temperature distribution, a 3-D hypothetical finite element model of concrete dam was developed. A transient heat transfer analysis was performed based on the recorded air temperature data of Cape Town for a period of 14 years. The influence of heat fluxes from air, sun, reservoir and foundation on the thermal response of the dam have been considered in the analysis.

The direct integration scheme of the first order finite element equations by using the finite difference method was used for the analysis of the transient heat flow process due to its efficiency and ease of implementation. The integration time step was determined based on the

cyclic nature of seasonal temperature variations. It was observed in the analysis after several trials that daily average scheme performs well for capturing the thermal response of the dam due to variable air temperature. An annual variation of the influencing parameters was therefore used to obtain the overall dam thermal response.

To ensure a rapid convergence of the cyclical thermal response of the dam-foundation system, with seasonal temperature variations precribed at the boundaries of the system, the initial condition was assumed as near to the mean annual temperature distribution of the dam as possible. The temperature distribution obtained from the steady-state analysis was later used to perform the transient thermal analysis analysis.

7.2 Conclusion

Based on the literature and results obtained from the finite element analysis by implementation of the proposed foundation model the following conclusions have been drawn from the study:

- Transient Fourier heat conduction model is only mathematical model used to describe the transient heat flow mechanism in concrete dam walls.
- Finite element method is most relaible solution technique to perform thermal analysis in concrete dams
- 1-D heat tranfer analysis can not give accurate results thermal analysis of concrete dams due to the fact heat flow occurs in the direction normal to the longitudinal section. Whereas 2-D thermal analysis may considered accurate enough, relaiblereults can only be achieved in the case of gravity concrete dams where solar radiation shares on the exposed surface of the dam don not vary. Thus 3-D thermal analysis is inevitable when dealing with concrete arch dams.
- The main environmental factors affecting the concrete temperature for dams in operation are air temperature, reservoir temperature, foundation temperature, solar radiation and wind velocity.
- Foundation temperature is influenced by geothermal heat and variable atmospheric temperature. What is however of concern to a dam engineer is the effect of variable

foundation temperature which occurs to a depth of 20 m below the surface to overall dam wall temperature distribution.

- A model for predicting variation in foundation temperature using measured air temperature in the absence of measured foundation temperature has been proposed. It is further stressed here that measured data if used would give a more reliable result and hence use of measured records of foundation temperature if available must be used.
- The temperature distribution obtained from the steady-state analysis has been found to give a very good estimate of initial temperature distribution of thedam when annual average temperatures are applied at the boundaries. This very good results can only be achieved if and only if the initial approximations are very close to the annual mean temperatures.
- From the model, high thermal gradients are observed to a depth of about (3 m) from the downstream face and near the crest of the dam. Maximum principal tensile stresses observed corresponds to regions of high thermal gradients for the days considered. It must be noted that, thermally induced tensile stresses may produce surface cracking that will not affect the structural resistance of the dam significantly. However, when water is able to penetrate through, then these surface cracks may be of a serviceability concern and in the most extreme cases the structural integrity of the dam system may be compromised.
- Thermal response results indicate that variable foundation temperature has negligible effect on the thermal response of the dam away from the dam-foundation interface with 9% increase recorded for an internal node (7 m) from foundation interface. This statement would mean yes it is possible to get relative good representative results when thermal analysis of the dam is carried out without including the foundation in the model (Sheibany and Ghammian, 2006; Leger et al. 1993)
- Variable foundation temperature is observed to influence the concrete temperature to approximately 30 m from the dam-foundation interface.
- Water level on the upstream face of the dam is found to significantly influence the average concrete temperature by more than 50 % when most part (nearly 75%) of the

upstream face is left exposed. Slightly higher tensile stresses are recorded for the same case.

- The water temperature is found to have a negligible effect on thermal response across the dam thickness compared to when exposed to air and solar radiation effects for the case studied. This is true because the presence of the reservoir insulates the upstream face of the dam and thus prevents the possible developments of large thermal gradients and associated thermal stresses near this face. The former statement does not aggree with the one reported by Sheibany and Ghaemian (2006) where in their study they found that water temperature influences the temperature distribution across the dam thickness more than air temperature

7.3 Recommendations for further research

- Perhaps the most crucial improvement to this study at its present state is a full scale implementation of the proposed foundation temperature model is needed in a real concrete dam finite element model and results correlated with those obtained from thermometric records embedded in the dam.
- Temperature thermal properties such as heat convection coefficient and thermal conductivity need to be considered to correctly simulate the heat transfer mechanism occurring in and at the dam boundaries
- Large measured data sets that reflect tha actual occurance need to be collected and analyzed to provide a better thermal and stress response for the different parameters investigated.
- The effect of spatially variable air temperature on downstream face of the dam needs to be investigated as it may affect thermal and stress response due to changes in dam orientation and variable dam heights
- Analysis of the effect of climate change on foundation temperature using the finite model of dam-foundation system is required to define extreme conditions which have never been experienced by the dam-foundation system. This would enable adequate dam safety evaluation measures to be taken

- Regression models need to be explored and their effectiveness in establishing the temperature distribution in concrete dams. These would provide cheap and easy alternative rather than the finite element method which requires a good deal of experience and knowledge to implement.

REFERENCES

[1] Daoudu, M., Galanis, N., and Ballivy, G. (1997). “Calculations of the Periodic temperature field in concrete dams.” Can. J. Civ. Eng., 24(5), 772-784.

[2] Leger, P., and Seydou, S. (2009). “A seasonal thermal displacements of gravity dams located in Northern regions.” J. Perf. Constr. Fac., 23(3), 1-9.

[3] Abdullah, M., Mutasha. S., and Tony, J.Q. (2003), “ Thermal structural modelling and temperature control of RCC Gravity dams.” J. Perf. Constr. Fac., 17(4), 177-187.

[4] Leger, P., Venturelli, J., Bhattacharjee, S.S. (1993a,b). “Seasonal temperature and stress distribution in concrete gravity dams.” Can. J. Civ. Eng., 20(6), 999-1017.

[5] Saetta, A., Scotta, R., and Vitaliani, R., (1995). “Stress analysis of concrete structures subjected to variable thermal loads.” J. Struct. Eng., 121(3), 446-457.

[6] Malla, S.,Wieland, M. (1999). “Analysis of an arch-gravity dam with a horizontal crack” Comput Struct, 72, 267–78.

[7] Ardito, R., Maier, G., and Massalongo, G. (2008) “Diagnostic analysis of concrete dams based on seasonal hydrostatic loading.” J. Mech Behaviour Mater, 15(6): 381–9.

[8] U.S. Army Corps of Engineering.(1994). “Arch dam design.” Engineer manual 110-2-220, Chap. 8, 1–15.

[9] Sheibany, F. and Ghaemian, M. (2006). “Effects of environmental action on thermal stress analysis of Karaj concrete arch dams” J. Eng. Mech., 132(5), 532-544.

[10] Bofang, Z. (1997). “Prediction of water temperature in deep reservoir” Dam Eng., VIII (1), 13–25.

[11] Agullo, L., Mirambell, E., and Aquado, A. (1996). “A model for the analysis of concrete dams due to environmental thermal effects” Int. J. Numer. Methods heat fluid flow, 6(4), 25-36.

[12] Léger, P. and Leclerc, M. (2007). “Hydrostatic, temperature, time-displacement model for concrete dams” J. Eng. Mech., 133(3), 267-277.

[13] Bofang, Z. (2003). “RCC arch dams: Temperature control and design of joints.” Int. Water Power Dam Constr., 55(80, 26–30.

[14] Engineering monograph, (1977). “Design Criteria for concrete arch and gravity dams” Vol. 19.

[15] Yoshida, H., Yamazaki, M., and Shibata, K., (1983). “An analytical study on the thermal stress of mass concrete” Part iv, The annual report of A IJ 110-117

[16] Janna, W., (1988). *“Engineering heat Transfer”*, SI Ed., Van Nostrand Reinhold (interntional), UK.

[17] Sabbagh-Yazdi, S.R. and Mastorakis, N.E. (2007). “3D heat generation and transfer in gravity dam on rock foundation using Galerkin Finite Volume solver on tetrahedral mesh” International Journal of Geology, 1(3), 52-60.

[18] U.S. Army Corps of Engineers (USACE). (1995).“Engineering and design; gravity dams.” *EM 1110-2-2200*, Washington, D.C.

[19] Tarbox, G. S. (1977). “Design of concrete dams.” *Handbook of dam engineering*, A. R. Golzé, ed.,Van Nostrand Reinhold Company, Toronto, Canada.

[20] Ishiguro, S. and Nakaya, M. (1986). “Temperature distribution analysis of concrete in fill dam gallery” Bull. Univ. Osaka, vol. 38, 35-43.

[21] De Sortis, A., and Paoliani., P. (2007). “Statistical analysis and Structural identification in concrete dam monitoring” Eng. Struct.,29, 110-120.

[22] Shun-wen, J., Yue-Ming, Z. and Sheng, Q. (2008).“Forecast of water temperature in reservoir based on analytical solution.” J. of hydrodynamics, 20(4), 507-513.

[23] Jesung, J., Jongwook, L., Donghoon, S., and Hangyu, P. (2009). “Development of dam safety management system” Advances in engineering software, 20, 554-563.

[24] Kook-Han, K., Sung-Eun, J., Jin-Keun, K., and Sungchul, Y. (2003). “An experimental study on thermal conductivity of concrete” Cement and Concrete research, 33, 363-371.

[25] Power, H.C. and Mills, D.M. (2005). “Solar radiation climate change over Southern Africa and an assessment of the radiative impact of volcanic eruptions” Int. J. Climatol.,25, 295-318.

[26] Ashna, N. and Koichi, F. (2001). “Three dimensional finite element analysis of a Roller Compacted Concrete (RCC) dam due to variable thermal loads” J. Civ. Eng. Bangladesh, 9(1), 65-85

[28] Kaufmann, K.W. and Ricardo, C.T. (2005). “Water Temperature Variation and the Meteorological and Hydrographic Environment of Bocas del Toro, Panama” Carribean Journal of Science, 41(3), 392-413.

[29] Smith, K. (1975). “Water temperature variations within a major river system” Nordic Hydrology, 6, 155-169

[30] Miguel, C., Javier, O., and Tomas, P. (2000).“Simulation of construction of RCC dams, Temperature and Aging” J. Struct. Eng., 126(9), 1053-1061

[30] Ning, L., Bin, H., and Zhi-Wen, Y. (2001).“Stochastic finite element method for random temperature in concrete structures” Int. J. of Solids and Struct., 38, 6965-6983

[31] Gosselin, C. and Mareschal, J.C. (2003). “Variations in ground surface temperature histories in the Thompson Belt, Manitoba, Canada” Global and Planetary Change 39, 271–284

[30] Flores, E.L., Prol-Ledesma, R.M., and Royer, J.J. (2001).“ Boundary conditions in thermal models: An application to a KTB site Germany” Geofisca Internacional., 40(2), 97-109

[31] Chalko, T. J. (2004). “Can Earth explode as a result of Global Warming?” NU J. of Discovery, 3, 1-9

[32] salah El-Din, T. J. (1999). “On the heat flow into the ground” Renewable Energy 18, 473-490

[33] Mihalakakou, G., Santamouris, M., Asimakopoulos, D., and Argiriou, A. (1995).“On the ground temperature below buildings” Solar Energy, 55(5), 355-362.So

[34] Beltrami, H. and Kellman, L. (2003). “An examination of short- and long-term air–ground temperature coupling” Global and Planetary Change 39, 271–284

[35] Beltrami, H. (2001). “On the relationship between ground temperature histories and meteorological records: a report on the Pomquet station” Global and Planetary Change 29,327–348

[36] Jones, P.D., Osborn, T.J., and Briffa, K.R. (2001).“ The Evolution of Climate Over the Last Millennium” Science, 292, 1-

[37] S.C. Chapra and R.P. Canale, (1998). “Numerical Methods for Engineers”, McGraw Hill, Boston, 3rd Edition

APPENDIX A:SOLAR RADIATION SHARES IN SOUTH AFRICAN MAJOR CITIES

Station	Long-term annual mean (W m^{-2})	Standard deviation of annual mean (W m^{-2})	Trend (W m^{-2} per decade)	Trend (% per decade)	Significance level (%)
Alexander Bay	191.8	7.1	−5.6 ± 3.6	−2.8	99.4
Bloemfontein	187.1	10.6	−2.9 ± 3.4	−1.5	90.4
Cape Town	159.7	8.4	−3.5 ± 2.5	−2.1	99.1
Durban	117.4	6.7	−2.0 ± 2.5	−1.7	89.4
Grootfontein	188.6	11.6	3.4 ± 8.3	1.8	59.1
Port Elizabeth	139.2	8.8	2.5 ± 3.7	1.2	81.1
Pretoria	161.6	9.1	−2.1 ± 2.3	−1.3	93.3
Upington	211.8	18.1	−1.9 ± 8.4	−0.9	35.2
Keetmanshoop	229.3	11.6	3.3 ± 5.9	1.5	74.2
Windhoek	208.6	11.7	−2.4 ± 5.7	−1.1	60.7
Mean	173.9	11.5	−4.8 ± 2.6	−2.6	99.9

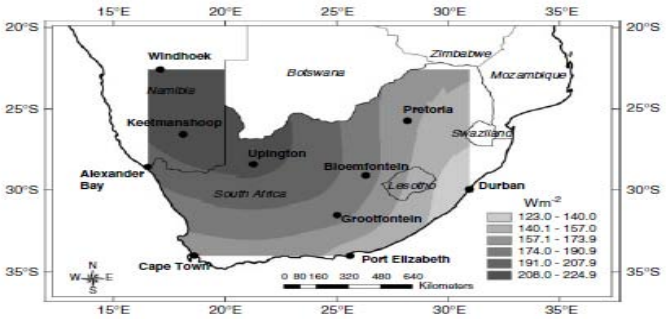

Fig.1: Annual averages for direct irradiation

Station	Variable	Jan	Feb	Mar	Apr	May	Jun	Jul	Aug	Sep	Oct	Nov	Dec
AB	Mean	271.1	243.7	206.6	161.4	129.8	108.9	114.7	141.3	173.3	216.7	263.4	269.4
	SD	21.0	21.1	12.6	12.1	13.0	10.9	9.9	11.5	19.1	17.6	17.1	14.5
	Trend	4.7	−8.2	−6.9	−0.6	5.7	−0.2	0.2	−0.8	**−12.2**	−5.2	−7.5	−3.8
BL	Mean	232.9	209.0	182.3	158.2	139.9	125.1	136.3	165.3	187.8	212.3	242.1	253.6
	SD	38.3	41.3	28.0	16.9	12.3	12.3	12.2	17.3	23.7	31.6	28.8	28.0
	Trend	−1.8	**−13.9**	−2.2	−3.2	1.5	0.6	1.2	−3.2	−6.1	−5.0	−1.8	−0.6
CT	Mean	258.3	234.4	189.8	123.8	80.0	64.4	72.8	95.3	130.5	184.2	235.6	255.3
	SD	20.1	18.1	15.9	16.3	15.7	12.1	12.4	12.4	20.3	18.2	23.8	27.1
	Trend	−2.1	−1.0	**−4.9**	−4.2	−2.3	−3.3	**−5.8**	−1.1	−5.2	2.1	−4.3	**−8.7**
DN	Mean	135.5	142.4	132.5	115.9	99.0	92.1	94.1	104.2	104.9	115.6	125.6	142.7
	SD	22.1	20.9	20.8	12.3	7.6	10.0	9.5	15.5	16.2	19.8	21.8	19.7
	Trend	−3.2	**−7.5**	−6.2	0.8	−1.5	**−3.7**	−1.3	**−5.3**	−3.1	−0.6	2.4	−3.9
GR	Mean	266.3	213.6	186.0	152.0	123.7	113.2	123.8	153.8	179.7	217.6	257.6	280.1
	SD	33.5	39.9	27.5	16.3	17.1	6.5	11.3	17.1	26.2	24.1	29.5	31.9
	Trend	15.8	8.9	11.1	1.7	9.7	0.1	2.6	−3.8	1.0	−2.6	−4.8	12.5
PE	Mean	195.5	177.8	146.7	117.0	91.8	80.6	87.4	106.2	124.2	156.2	182.3	208.9
	SD	23.7	20.2	16.6	12.8	10.1	10.4	10.5	12.7	20.7	24.4	19.9	18.9
	Trend	−3.7	−1.9	−3.1	−3.2	−1.8	−2.0	−1.6	−1.1	−3.0	−5.2	−4.2	−3.8
PR	Mean	175.3	165.8	154.4	145.0	141.0	130.0	137.2	160.5	179.7	183.7	179.6	187.6
	SD	30.1	34.3	29.1	22.5	14.0	10.4	11.3	14.4	25.8	25.0	25.0	24.9
	Trend	−1.4	−6.6	−5.0	2.3	−1.3	1.3	0.5	−3.5	−4.5	−6.2	−1.0	0.0
UP	Mean	286.2	246.1	209.5	171.3	147.6	126.9	140.1	167.4	201.7	237.5	282.3	293.8
	SD	36.2	31.2	16.6	17.6	11.1	8.9	8.8	14.5	16.4	21.3	22.5	29.1
	Trend	6.4	−5.6	1.6	−1.6	1.0	−0.9	−2.6	−4.4	−3.1	−4.8	**−11.6**	1.1
KM	Mean	291.6	255.1	225.2	206.3	170.4	150.4	159.1	190.3	220.6	260.9	300.8	313.4
	SD	34.8	28.3	19.2	14.0	10.6	11.2	11.0	15.1	18.8	23.1	25.3	21.8
	Trend	4.1	−4.8	2.4	−2.2	−0.2	2.9	0.9	0.4	−2.0	3.8	11.6	7.9
WH	Mean	209.8	197.5	183.1	192.0	189.4	174.8	185.1	206.5	224.6	240.1	243.5	250.8
	SD	37.7	35.0	30.7	22.6	12.6	11.1	11.9	15.7	20.4	27.8	35.2	30.4
	Trend	−10.5	−9.7	−0.1	−7.4	−2.4	−4.0	0.4	−0.9	−3.1	−0.3	13.5	−6.5

Fig.2: Monthly averages for direct irradiation

Station	Long-term annual mean (W m^{-2})	Standard deviation of annual mean (W m^{-2})	Trend (W m^{-2} per decade)	Trend (% per decade)	Significance level (%)
Alexander Bay	61.2	3.1	1.8 ± 1.8	3.1	94.3
Bloemfontein	59.6	4.9	−1.5 ± 1.6	−2.4	93.9
Cape Town	61.4	4.2	0.2 ± 1.4	0.4	26.1
Durban	69.9	4.0	0.4 ± 1.5	0.6	39.5
Grootfontein	54.5	3.8	**−3.0 ± 2.4**	**−5.2**	**98.3**
Port Elizabeth	68.6	6.4	**−3.1 ± 2.5**	**−4.2**	**98.1**
Pretoria	68.1	5.5	−1.1 ± 1.4	−1.6	89.2
Upington	50.2	3.5	−0.8 ± 1.6	−1.6	70.2
Keetmanshoop	50.6	6.5	0.3 ± 3.4	0.5	12.8
Windhoek	61.0	7.0	−0.5 ± 3.4	−0.9	24.3
Mean	61.8	4.9	0.0	0.0	0.9

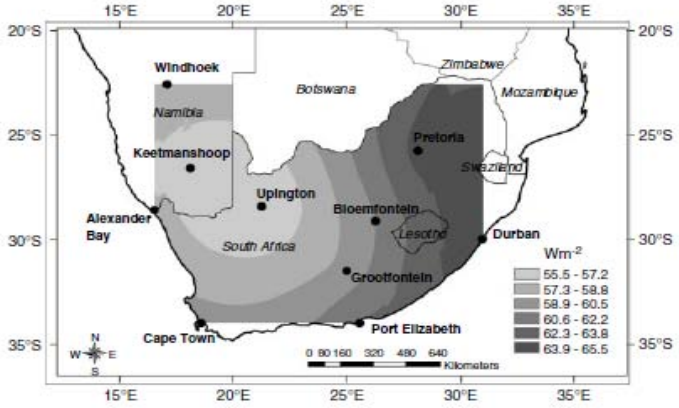

Fig.3: Annual averages for diffuse irradiation

Station	Variable	Jan	Feb	Mar	Apr	May	Jun	Jul	Aug	Sep	Oct	Nov	Dec
AB	Mean	76.3	71.7	61.7	50.3	42.4	39.3	42.0	52.2	67.1	76.4	77.4	80.9
	SD	8.7	8.4	6.4	5.1	4.9	5.2	4.6	6.3	8.5	8.0	7.9	5.8
	Trend	−1.5	4.4	**4.0**	−0.1	−2.1	0.8	0.6	1.6	**5.8**	1.1	3.7	1.5
BL	Mean	85.0	78.1	67.0	49.9	36.4	31.2	32.7	40.9	59.6	73.8	79.1	81.1
	SD	13.7	12.7	10.7	6.5	5.9	5.7	6.0	7.5	8.1	12.4	11.3	10.9
	Trend	−1.5	1.0	−2.9	−0.6	**−3.0**	**−2.3**	**−2.2**	−1.6	−0.3	−1.2	−0.8	−2.5
CT	Mean	76.7	67.3	57.2	50.0	42.5	36.1	38.3	50.0	67.1	78.4	83.9	83.3
	SD	9.4	8.9	7.0	6.1	5.4	3.9	3.9	5.1	8.0	8.5	9.9	10.7
	Trend	−0.3	−0.8	0.0	−0.3	−0.3	−0.9	0.3	0.2	0.5	−0.9	1.4	2.2
DN	Mean	103.0	90.2	74.5	54.7	41.3	34.5	38.6	50.4	68.5	85.3	98.6	105.1
	SD	8.6	9.2	7.5	5.8	4.3	4.4	4.6	4.7	5.5	6.7	7.6	9.1
	Trend	0.3	3.0	0.7	−0.2	0.6	0.2	0.5	0.8	0.5	−1.5	0.5	3.0
GR	Mean	72.9	72.0	59.3	46.7	35.1	29.8	30.7	39.0	58.9	67.9	73.8	69.4
	SD	12.4	14.5	7.0	6.8	6.1	2.6	3.9	4.0	6.6	9.6	10.4	8.7
	Trend	−6.5	−5.0	−4.0	−3.5	−2.1	−0.9	−1.5	1.2	−1.3	−0.7	0.5	**−7.7**
PE	Mean	98.8	87.5	70.3	52.8	39.6	33.2	35.8	47.8	70.6	87.9	101.9	100.4
	SD	14.1	11.3	9.1	5.9	4.3	4.4	4.9	5.9	8.0	10.5	9.9	8.7
	Trend	−3.7	−1.9	−3.1	**−3.2**	**−1.8**	**−2.0**	−1.6	−1.1	−3.0	**−5.2**	**−4.2**	**−3.8**
PR	Mean	101.8	94.1	78.8	57.3	40.3	35.4	37.4	45.9	60.8	76.5	91.8	98.3
	SD	12.4	13.2	10.2	10.1	6.2	5.3	5.5	6.0	8.2	11.9	11.5	12.3
	Trend	−1.9	−0.5	−1.1	−1.0	−0.3	−1.3	−1.2	−0.3	0.1	0.4	**−3.2**	−2.5
UP	Mean	61.7	63.5	56.2	45.7	33.1	30.8	30.7	40.5	53.1	64.6	62.0	59.4
	SD	13.8	11.7	7.8	6.5	6.5	4.8	4.3	5.8	8.3	7.2	9.9	9.8
	Trend	−5.8	−0.1	−2.9	−0.5	−1.5	−0.6	−0.4	0.2	−1.6	0.8	4.2	−3.0
KM	Mean	66.9	66.8	56.1	40.1	33.8	31.4	32.7	40.5	55.0	61.6	60.2	60.8
	SD	13.7	12.8	8.2	7.1	5.8	6.2	6.4	9.5	12.1	10.0	11.0	10.9
	Trend	−0.6	2.0	0.3	0.6	−0.7	−1.3	−0.4	1.3	3.3	−0.9	−3.4	−2.5
WH	Mean	92.9	86.9	77.1	51.6	32.3	28.9	29.3	40.2	57.3	70.2	78.6	79.6
	SD	12.7	11.5	11.1	9.5	6.0	5.8	7.5	8.4	10.7	12.2	13.4	11.3
	Trend	1.3	0.9	−2.2	−0.9	−2.1	−0.9	−2.2	−2.1	−1.7	−4.3	**−8.3**	−3.9

Fig.4: Monthly averages for diffuse irradiation

	Lat. (°S)	Lon. (°E)	Elevation (m)	Period	Length (years)
South Africa					
Alexander Bay	28.57	16.53	21	1958–83	26
Bloemfontein	29.10	26.30	1351	1957–91	35
Cape Town	33.97	18.60	44	1958–94	37
Durban	29.96	30.95	8	1957–90	34
Grootfontein	31.48	25.03	1270	1969–89	21
Port Elizabeth	33.98	25.60	60	1958–89	32
Pretoria	25.73	28.18	1330	1957–97	41
Upington	28.40	21.27	836	1965–92	28
Namibia					
Keetmanshoop	26.57	18.12	1066	1957–82	26
Windhoek	22.57	17.10	1725	1957–83	27

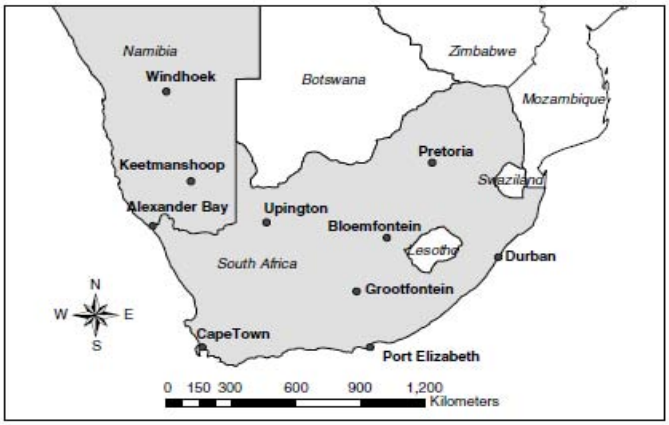

Fig.5: Global irradiation

Station[2]	Variable[3]	Jan	Feb	May	Apr	Mar	Jun	Jul	Aug	Sep	Oct	Nov	Dec
AB	Mean	349.7	315.9	270.1	212.1	172.2	148.1	157.2	194.0	243.3	293.2	341.0	351.4
	SD	15.6	13.4	9.9	8.3	9.0	7.0	7.0	7.8	16.3	10.4	10.4	10.7
	Trend	7.0	−3.1	−2.5	0.1	3.3	0.6	1.4	1.5	−5.8	−3.3	−2.6	−0.4
BL	Mean	317.8	287.1	249.2	208.1	176.3	156.2	168.9	206.1	247.4	286.1	321.1	334.7
	SD	27.6	32.5	20.7	13.8	8.5	9.3	9.0	13.5	18.8	22.5	20.8	22.7
	Trend	−3.3	**−13.0**	−5.1	−3.8	−1.5	−1.7	−1.0	**−4.8**	**−6.4**	−6.2	−2.6	−3.0
CT	Mean	335.1	301.7	247.0	173.6	122.5	100.9	111.1	145.1	197.2	262.2	319.0	338.2
	SD	14.0	12.2	11.6	13.7	11.5	10.7	11.3	11.1	14.7	12.3	17.1	19.2
	Trend	−2.4	−1.9	**−4.9**	**−4.6**	−2.6	**−3.6**	**−5.5**	−1.1	**−5.1**	0.6	−2.3	**−5.9**
DN	Mean	238.6	231.9	206.6	170.4	140.3	126.8	133.1	154.7	173.6	201.0	224.4	246.6
	SD	16.7	17.6	17.1	8.9	7.2	8.1	7.3	14.3	16.9	17.8	21.0	19.8
	Trend	−2.9	−3.0	−5.8	0.3	−0.9	**−3.6**	−1.2	−4.5	−2.7	−2.1	3.2	−2.9
GR	Mean	339.2	285.6	245.3	198.7	158.7	143.0	154.5	192.9	238.5	285.5	331.4	349.5
	SD	23.9	28.6	22.7	11.3	13.4	5.3	9.4	14.1	21.7	19.4	22.8	27.0
	Trend	9.4	3.9	7.1	−1.8	7.6	−0.8	1.1	−2.6	−0.3	−3.4	−4.3	4.8
PE	Mean	294.8	265.1	216.9	169.8	131.4	113.7	123.2	154.1	194.4	243.9	283.6	309.4
	SD	14.7	13.2	11.9	9.5	7.6	7.2	6.9	8.2	15.7	17.7	14.5	15.0
	Trend	1.1	−4.3	−0.1	−0.5	0.9	−0.7	−0.5	−1.1	−2.1	−0.1	−4.9	−4.9
PR	Mean	276.1	259.8	233.2	202.4	181.3	165.4	174.6	206.4	240.5	260.2	271.3	285.9
	SD	22.7	24.9	22.7	16.4	9.5	7.1	7.8	11.4	20.6	17.9	19.3	18.5
	Trend	−4.3	**−7.1**	**−6.0**	1.3	−1.6	0.1	−0.7	**−3.7**	−4.4	**−5.8**	−4.2	−2.4
UP	Mean	346.6	309.2	264.8	217.6	180.6	158.8	170.3	208.2	253.7	303.5	345.0	353.7
	SD	24.2	21.8	12.6	12.5	5.8	6.3	7.0	10.0	12.3	15.4	15.0	22.2
	Trend	0.9	−7.6	−1.2	−1.8	−0.4	−2.2	−3.0	−4.3	**−5.5**	−3.2	**−8.1**	−2.3
KM	Mean	357.7	321.9	281.3	245.5	204.2	181.8	192.2	230.6	275.6	322.5	360.9	374.2
	SD	24.6	20.5	14.2	10.5	7.3	6.8	7.1	8.5	9.7	14.9	18.6	15.6
	Trend	2.6	−2.8	2.7	−2.7	−0.9	1.6	1.1	1.8	1.3	2.9	8.2	5.4
WH	Mean	303.9	284.4	261.9	243.9	221.6	203.1	213.7	246.0	281.3	310.7	322.0	329.4
	SD	27.3	25.6	21.2	14.7	8.6	7.6	7.6	9.7	11.9	18.8	24.8	22.4
	Trend	−6.6	−8.8	−0.5	−6.9	**−4.4**	**−5.5**	−2.4	−3.7	−5.2	−3.6	6.2	−7.2

Fig.6: Statistical analysis for global irradiation

Station	Long-term annual mean (W m^{-2})	Standard deviation of annual mean (W m^{-2})	Trend (W m^{-2} per decade)	Trend (% per decade)	Significance level (%)
Alexander Bay	254.6	6.9	-0.6 ± 3.8	−0.2	23.4
Bloemfontein	246.6	9.5	$\mathbf{-4.4 \pm 2.8}$	**−1.7**	**99.7**
Cape Town	221.1	6.4	$\mathbf{-2.8 \pm 1.8}$	**−1.3**	**99.7**
Durban	186.9	7.6	$\mathbf{-2.6 \pm 2.5}$	**−1.4**	**96.0**
Grootfontein	243.2	10.1	0.4 ± 7.3	0.2	8.6
Port Elizabeth	208.2	5.6	-1.5 ± 2.1	−0.7	85.0
Pretoria	229.8	7.4	$\mathbf{-3.3 \pm 1.6}$	−1.4	**100.0**
Upington	259.8	8.0	$\mathbf{-4.0 \pm 3.4}$	−1.5	**97.7**
Keetmanshoop	278.0	8.0	1.7 ± 4.1	0.6	59.9
Windhoek	268.2	8.0	-3.4 ± 3.7	−1.2	92.2
Mean	234.5	9.1	$\mathbf{-5.4 \pm 1.6}$	**−2.2**	**100.0**

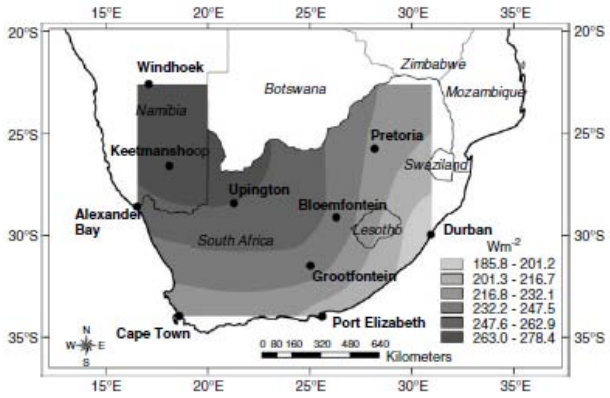

Fig.7: Annual average for global irradiation